ERDF project No. 1.1.1.5/2/24/A/004

The 6th International Biennial Conference

Photonics Sciences and Space Research – Riga 2025

22–23 April 2025, Riga

Presentation Abstracts

Tuesday, April 22

Space Photonics and Astrophysics

Invited Keynote presentations 1

Online **Bernard Foing.** ***ERA Chair at NSP FOTONIKA-LV***
Space photonics for Moon & Mars exploration

Andris Vaivads. ***Rector, Ventspils University of Applied Sciences***
Plasma energization in the solar wind and the Earth's magnetosphere

Plenary session 1

Arnolds Ūbelis, Aigars Atvars. ***University of Latvia***
Development of NSP FOTONIKA-LV boosted by two ERA Chair projects

Kalvis Salmiņš. ***University of Latvia*** and **V. Bespaļko,** ***Eventech Ltd***
Data Acquisition Full Record Mode in Satellite Laser Ranging

Ilgmārs Eglītis, Kristers Nagainis. ***University of Latvia***
The perspectives of research on small bodies of the solar system in Baldone Observatory

Online **Harald Hiesinger, Bastian Gundlach.** ***University of Münster***
Contribution of University of Münster research teams in research on meteorites, asteroids, and comets

Dmitrijs Bezrukovs, ***Ventspils International Radio Astronomy Centre***
Prospects and Problems of Microwave Observations of the Sun with RT-32 Radio Telescope

Online **Ivan L. Andronov,** *et al*. ***Odesa National Maritime University***, *et al*
Multi-harmonic and special shape/pattern/template approximations of discrete signals with generally irregular arguments

Plenary session 2

Online **Sergey Kravchenko.** ***Cryogenic and Vacuum Systems, Ltd***
Advancing space simulation equipment for comprehensive testing of payloads

Ashish Kumar Singh, Anatolijs Sharakovskis, Reinis Ingantans, Meldra Kemere, Arnolds Ūbelis. ***University of Latvia***
Experimental and First Principles Analysis of Dielectric and Optical Properties of Magnesium Alloys

Juulia-Gabrielle Moreau. ***Marie Curie fellowship, University of Latvia***
Experimentally induced darkening of dunite, a small step in understanding more about asteroid interlopers

Janis Kaminskis. ***Riga Technical University***
Gravity measurements in Latvian territorial waters and their future prospects

Online **Maria Teresa Belmonte, Pratyush Ranjan Sen Sarma, Santiago Mar.** ***University of Valladolid***
Plasma emission spectroscopy and its role in the study of the origin of heavy elements

Sergejs Boroviks. ***Swiss Federal Technology Institute of Lausanne***
Quantum and nonlinear plasmonics on crystalline gold surfaces

Poster session

- **Aigars Ciniņš,** ***University of Latvia***. Coherent manipulation of quantum states using the Autler-Townes effect
- **Aleksandrs Koļesņiks, Arnolds Ūbelis, Austris Pumpurs,** ***University of Latvia.*** Application of resonance atomic spectra lines of Se I and Te I in measurement transmittance of optical fibers in far UV

- **Arman Bzhishkian, Janis Blahins, *University of Latvia***. Dirac Delta pulse generator – powerful tool for diagnostics in electronics
- **Arnolds Ūbelis, Austris Pumpurs, Jānis Kļaviņš, Arman Bzhishkian, Jevgenijs Gabrusenoks, *University of Latvia***. Measurement of atomic and ionized (B I and B II) spectra of hardly volatile Boron using unique technique - hybrid plasma system
- **Arnolds Ūbelis, Zane Mētra, Aleksandrs Koļesņiks, *University of Latvia*** and **Jānis Rupkus, *Riga Photonics Centre***. Measurement of atomic and ionized (Pb I and Pb II) spectra of Lead hybrid plasma system
- **Inga Brice, *University of Latvia*** and **Arvīds Sedulis**, **Janis Alnis, *University of Latvia*** and ***Riga Technical University***. Exploring optoplasmonic doped whispering gallery mode microspheres
- **Jānis Blahins, *University of Latvia***. On current status of small sized innovative boron ion implantation apparatus
- **Kalvis Kalniņš, Uldis Bērziņš, *University of Latvia*** and **Vyacheslav V. Kim, Rashid A. Ganeev**, ***Institute of Fundamental and Applied Research National Research University***. Formation of LIPSS on GaAs in water using radially and azimuthally polarized laser beams
- **Kristers Nagainis, *University of Latvia*** and **Michele Moresco, Massimo Guidi, Antonio Farina, Alfonso Verapolumbo** (***Italy***). Machine learning solution for enabling cosmological analysis with the matter anisotropic three-point correlation function
- **Kristians Draguns, Jānis Alnis, *University of Latvia.*** Tantalum pentoxide microring resonators
- **Krišjānis Krakops, *NSP FOTONIKA-LV***. The firms that break light. A summary of statistics of the Photonics and Optics industry in Latvia in the last 5 years
- **Matīss Čakšs, Arnolds Ūbelis, Aleksandrs Koļesņiks, Juris Silamiķelis*, University of Latvia*.** Spectroscopic studies of Gd I and Gd II using hybrid plasma source
- **Uldis Bērziņš, Arturs Ciniņš, *University of Latvia***. Measurements of metastable ion lifetimes
- **Victor Kärcher, Tobias Reiker, *Center for Soft Nanoscience, Germany*** and **Pedro F.G.M. da Costa, *São Carlos Institute of Physics, Brazil*** and **Andrea S.S. de Camargo, Helmut Zacharias, *Friedrich-Schiller University Jena***. Coherent control in size selected semiconductor quantum dot thin films
- **Viesturs Silamiķelis, Aigars Apsītis, Jānis Blahins, Austris Pumpurs, Jānis Sniķeris, Ashish Kumar Singh, *University of Latvia*.** The effect of EM levitation, pressure and temperature combination on synthesizing the Magnesium – high Titanium alloys
- Online **Pratyush Ranjan Sen Sarma, María Teresa Belmonte, Santiago Mar, *University of Valladolid***. Investigating the impact of hollow cathode lamp geometry on neodymium emission spectra

Wednesday, April 23

Photonics Sciences

Invited Keynote presentations 2

Online **V.V. Kim, *Institute of Fundamental and Applied Research under the National Research University*** and **Rashid Ganeev, *ERA Chair at NSP FOTONIKA-LV***
Generation of XUV vector/vortex beams in laser induced plasmas

Online **Sune Svanberg. *Lund University***
Interdisciplinary Laser Spectroscopy - The interplay between basic and applied sciences and resulting industrial impact

Plenary Session 3

Jānis Alnis. *University of Latvia*
Levitation of WGM microspheres: optical, electrodynamic, magnetic

Uldis Bērziņš. ***University of Latvia***
Laser Spectroscopy of Negative Ions

Arnolds Ūbelis. ***University of Latvia***
Advances in Application of Hybrid system: Hollow Cathode and Low Temperature Inductively Coupled Plasma for Spectroscopic Investigation of Basic Properties of Atoms and Ions of Hardly Volatile Elements

Online **Henrik Hartman.** ***Malmö University***
Laboratory Atomic Spectroscopy for stellar and kilonova astrophysics

Richard Thomas. ***Stockholm University***
Probing molecular mutual neutralization reactions of atmospheric importance using the ion storage facility DESIREE

Jyrki Saarinen. ***University of Eastern Finland***
Entrepreneurship and photonics innovations, case of Finland

Plenary session 4

Online **A.N.K. Reddy, H. Zacharias, H. Yilmaz, V.V. Kim, V. Kärcher, V. Anand, R.A. Ganeev.** ***University of Münster***
Generating high-harmonic array beams

Online **Vyacheslav Kim, Rashid Ganeev, Arnolds Ūbelis, Dainis Ozols.** ***University of Latvia***
The application of laser-induced breakdown spectroscopy for analysis in ores from deep boreholes in Latvia

Lev Nagli, Kirill Kulikov, Dima Cheskis, ***Ariel University***
Four-level Generation in Laser-Induced Plasma Lasers

Online **Ulises Miranda.** ***BSI Ltd***
Quantum Mechanical Calculations of molecular Dimers of Heavy Elements

Online **Petro Smertenko, Vadym Naumov, Zinoviia Tsybrii, Ihor Lysiuk, Daria Kuznetsova,** ***Institute of Semiconductor Physics, National Academy of Sciences of Ukraine*** and **Arnolds Ūbelis,** ***NSP FOTONIKA-LV, University of Latvia***
Towards the use of organic materials in the terahertz range

Online **Vadym V. Korotyeyev, Pavlo Sai, Viacheslav V. Kochelap.** ***Institute of High Pressure Physics PAS*** and ***V. Ye. Lashkaryov Institute of Semiconductor Physics, NASU***
Plasmonic crystals for THz applications

Online **Jurģis Grūbe, Kalvis Alps, Mārtiņš Narels, Ivo Brūvers**. ***Light Guide Optics International SIA***
Lightguide fiber bundles

Vladimir Gostilo. ***Baltic Scientific Instruments***
Research driven SMEs - Baltic Scientific Instruments Ltd: 30 years' experience in global markets

ERDF project No. 1.1.1.5/2/24/A/004

INTRODUCTION

FOTONIKA-LV: National Centre of Excellence for Photonics Sciences and Space Research

Arnolds Ūbelis

NSP FOTONIKA-LV, University of Latvia, Latvia

e-mail: arnolds@latnet.lv

The **National Science Platform FOTONIKA-LV** (NSP FOTONIKA-LV, http://fotonika-lv.eu/) currently incorporates 5 labs dealing with photonics sciences, and 2 observatories: the Astrophysical and Fundamental Geodynamic observatory[1] performing world-wide demanded observations and space research. Benefiting from the joint success of the integrated units in competitive calls of EU framework programmes, NSP FOTONIKA-LV has reached the level of a national scale centre of excellence. Targeting the European Research Area scaling is a response to the national vision and strategy[2].

NSP FOTONIKA-LV in quantum sciences, space sciences and technologies is the result of bottom-up action, and emerged as an Association FOTONIKA-LV (see Fig. 1) of three research institutes at the University of Latvia aiming at boosting jointly large projects in photonics sciences and technology in Latvia and lining with EC policy defining photonics among the leading six key enabling technologies in Europe (October 2009[3]). It is worth mentioning, that photonics sciences and space research were historically strong and visible in the landscape of the science and innovation in Latvia since 1960.

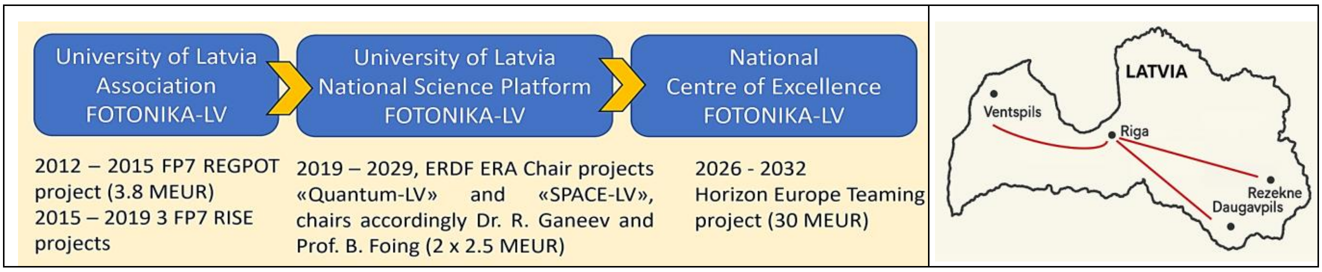

Figure 1**. History of the advancement of FOTONIKA-LV towards **NCoE FOTONIKA-LV with national-wide coverage

Photonics sciences, space research and observations, and relevant interplays within the domains have been on focus of the NSP FOTONIKA-LV since its founding and are key priorities in the EU. Photonics is included in the RIS3 strategies of Latvia and is foreseen as very important in the process of transformation of the national economy. Photonics is a basis for the impressive industry.

[1] having an advanced SLR station: ILRS code RIGL1884: International Laser Ranging Service: has ranking among 12 from more than 70 in the network: https://ilrs.gsfc.nasa.gov/network/stations/active/RIGL_station_info.html

[2] Guidelines for Science, Technology development and Innovation 2021-2027 (in Latvian), https://www.izm.gov.lv/lv/media/11967/download

[3] Willner, *et a*l. Optics and Photonics: Key Enabling Technologies. Vol. 100, 13 May 2012 | Proceedings of the IEEE

Particularly, the European Photonics Industry Consortium - EPIC[4] is formed from more than 850 companies; NSP FOTONIKA-LV of the University of Latvis is a member of the EPIC.

The envisioned emerging **National Centre of Excellence FOTONIKA-LV** (NCoE FOTONIKA-LV) is foreseen as a flagship in photonics sciences and space research in Latvia and across the Baltic countries, well recognised in the ERA, the driver of further structural changes, particularly advocating for Pan-Baltic regional smart specialisation (RIS3) in photonics sciences and space research to empower national and regional excellence to the standards of ERA. The focus of the Centre will be on ensuring advanced science, and interplay between two areas where scientists, researchers and professionals, possessing the same or similar education and background knowledge.

Prepared after Dr. Arnolds Ūbelis presentations

[4] European Photonics Industry Consortium (EPIC): https://epic-photonics.com

ERDF project No. 1.1.1.5/2/24/A/004

The perspectives of research on small bodies of the solar system in Baldone Observatory

Ilgmārs Eglītis, Kristers Nagainis

Institute of Astronomy, FST, University of Latvia

e-mail: ilgmars.eglitis@lu.lv

Observations

At the Baldone Astrophysical Observatory, astronomers operate with a Schmidt-type 1.2-meter telescope installed with two similar STX-16803 and Aluma AC4040 cameras in its focal plane. The brightness limit in the visual range of the telescope without a filter is 22 magnitudes at night with good transparency and calm images. CCD parameters: quantum effectivity 80%; the size of one pixel is 9 * 9 microns; and linear size 4096*4096 pixels, which corresponds to 53*53 arcmin of the field of view.

Achievement

The results from the monitoring of asteroids during 2008 – 2023 gave 149 new discoveries. The most important discoveries were Apollo-type N428694 = Saule (0.058 AU) and Centaur- type N330836 = Orius (12.44 AU).

type N330836 = Orius (12.44 AU).

Table 1. *The asteroids discovered and named asteroids st the Baldone Observatory*

Asteroid Nr	Name	Year of award the name
274084	Baldone	2011
284984	Ikaunieks	2012
330836	Orius	2013
332530	Canders	2015
352646	Blumbahs	2015
428694	Saule	2016
457743	Balklavs	2017
545619	Lapuska	2021
604750	Marisabele	2022
567580	Latuni	2022
598895	Artjuhs	2023
658787	Alksnis	2024

"Asteroid N635478 has been named "Fotonikalv" in recognition of the achievements of National Science Platform FOTONIKA-LV at the University of Latvia (founded in 2010) towards the consolidation of human capital in quantum sciences, space sciences, and technologies, to boost national progress and to be a strong partner in international consortiums contributing to implementation of the EU space strategy" - name awarded in 2024.

Asteroid monitoring future prospects

Problem: Observing near-Earth Objects (NEOs) holds significant importance for planetary defense, solar system formation studies, and resource mining applications. While meter-size or smaller NEOs harmlessly disintegrate in the Earth's atmosphere, larger ones can cause devastating damage. NEOs smaller than 140 m constitute a much larger population because their smaller sizes require closer proximity to Earth to be sufficiently bright for observation. The associated trailing loss from the faster motion rate becomes a substantial hurdle for surveying small hazardous NEOs.

Solving:

- synthetic tracking method by summarizing images with an exposure time short enough to prevent significant asteroid especially NEO motion relative to the size of the CCD pixels,
- need to determine the ideal exposure time for the number of frames,
- influenced by the system's hardware configuration,
- influenced by the sky background level,
- evolve the operational strategies by the different quality of transparency and turbulence of the atmosphere.

Present study of asteroid characteristics

Starting point for research of characteristics of asteroids, especially with small Earth MOID distances:

1. Baldone Observatory observations of selected asteroids in series compounded more than a hundred 180 or 240 sec. expositions, to achieve a signal-to-noise ratio greater than 20. Baldone observations are long time (2-4h) two-four night series with an accuracy of 0.05m.

2. Minor Planet Center position/magnitude archive data collected many milliard observations from 1934 in different observatories, in different passbands. Collected observations have short brightness measurement series unevenly scattered over a long-time interval with less accuracy (often 0.1 mag.) but with good statistics (from 1000 to 3000 observations from different observatories per asteroid).

The list of observable asteroids was compiled using the links of the Minor Planet Center MPC checker and MPC light curve database. The list included those NEO and main belt asteroids with Earth MOID distance less than 1.3 and a brightness greater than 18 magnitudes without period data. Observations of selected asteroids are usually made on three to five following nights. Three to five hours long series of observations were made for each asteroid. On average, it takes about more than a hundred observations for each object. Observations were made in the period 2020-2025 mainly with exposures of 180 or 240 sec, to achieve a signal-to-noise ratio greater than 20.

A methodology has been developed for determining the rotation period using the short brightness measurement series unevenly scattered over a long-time interval with low accuracy using a statistically large sample of brightness measurements [1]. The main methodological requirements for the data are that the number of observations in the series must be greater than 70, the common observation sample for the asteroid under study must be greater than 1000, the light curve obtained by the Lomb-Scargle (L_S) method must give two maxima and minima in one rotation cycle, the form of the power spectra peaks must be similar to Gaussian and the average value of the power spectra peak for the sample must be greater than 0.28. The rotation periods for 30 main-belt asteroids, mostly with Earth-MOID distances less than 1.1 AU, have been determined using the developed methodology and published brightness data from 19 different observatories.

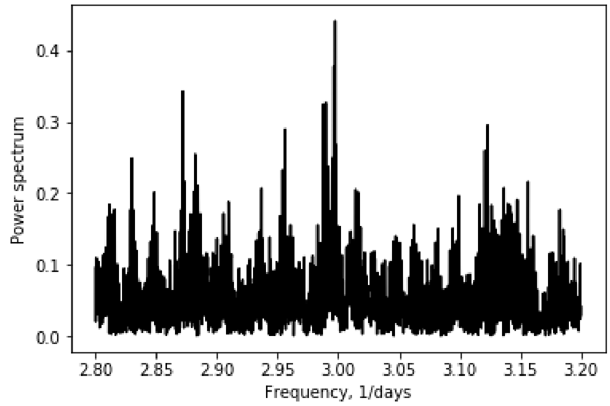

Figure 1. *L_S power spectrum of asteroid N3081 from Mauna Loa Observatory data*

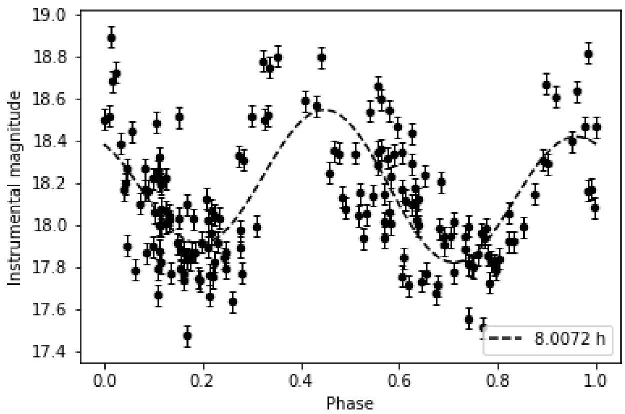

Figure 2. *Light curve for asteroid N3081 from Mauna Loa Observatory data*

Obtaining a common phase diagram

Data merging problem:

- brightness from different instruments (observatories),
- magnitudes in different passbands,
- measurements in different sky conditions,
- magnitudes processed using different catalogues,
- brightness bias is obtained using reference stars including those bluer than the Sun.

To obtain a common phase diagram for accuracy analyse the need:

- all brightness data are reduced to 1 AU,
- all brightness data are reduced to V magnitude,
- at the first iteration Hoffman et al.,2025 [3] bias values are used,
- certain types of asteroids have their specificities, so a brightness bias test is performed by combining all measurements from different observatories. The minimal discrepancy between observatory data is searched. The bias values for passbands B, g, c, V, w, r, R, G,

o, I, C for 106 S-type asteroids is obtained. It gives the possibility to construct a common phase curve from whole 19 observatories' brightness measurements for further analysis.

Period calculations from common phase diagrams

Results from Lomb-Scargle analysis of common phase diagram for asteroids with small dispersion (R2>0.7) and with average dispersion around phase function (0.4<R2<0.6):

Table 2. *Comparing rotation periods from previous methodology and common phase curve analysis*

Asteroid	Pcommon, h	Paverage, h	Error, %
3173	45.982	46.008	0.26
3473	9.074	9.074	0.15
3716	10.474	10.456	0.13
2607	2.936	3.015	1.03
2968	4.56	4.585	0.26
2971	4.491	4.495	0.35
3081	8.007	8.007	0

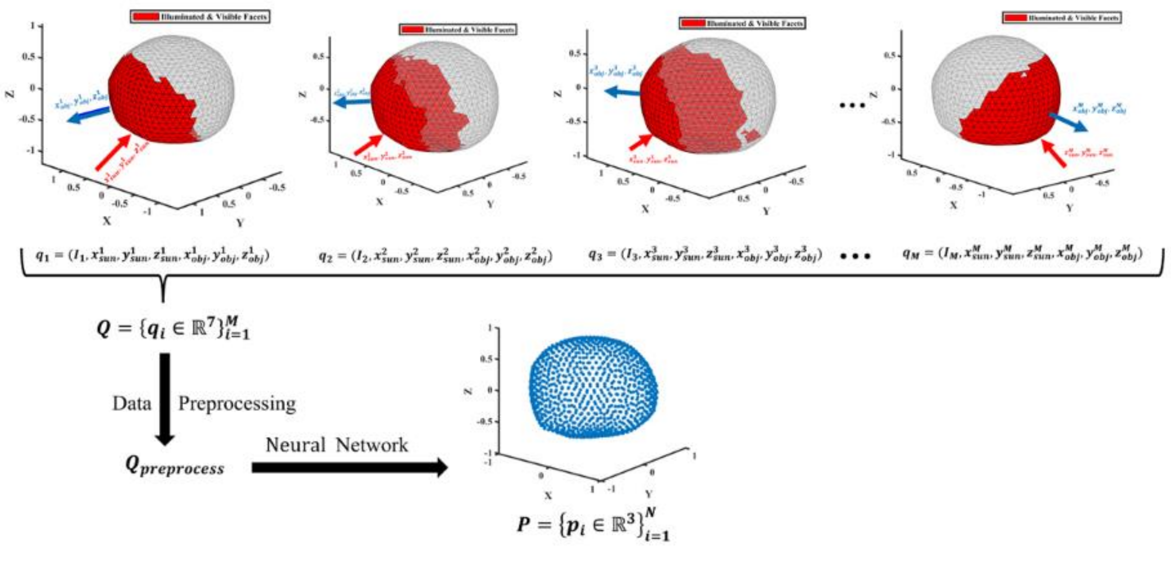

Figure 3. *Illustration of inversion method. The top four panels show the schematic diagrams of different visible and illuminated facets of the asteroid under varying Sun-asteroid-Earth positional relationships in the asteroid's body coordinate system. The blue point cloud represents the asteroid point cloud obtained from the inversion process*

Future perspectives to analyse common phase and light curves

The inversion of asteroid shapes from light curves fundamentally relies on the geometric relationships between the observer, the Sun, and the asteroid's surface. At a certain observation moment t_i, the brightness I_i of the asteroid is observed, and the direction vector of the Sun in the asteroid's body. Recording the brightness at time t_i along with the normalized direction vectors of the Sun and the observatory in the asteroid's body coordinate system yields a vector representation. The collection of observation vectors at various historical moments forms a set of Q. The goal of the algorithm is to establish the mapping P from the Q set. However, for this, we must know the parameters of rotation axis direction, rotation period, and phase function. That is the next step to solve this problem.

Acknowledgments: This research was supported by ERDF project Nr. 1.1.1.5/2/24/A/004.

References

[1] Eglitis I., Svincicka D. (2025) Rotation period estimates for 14 asteroids with the Earth MOID less than 1.1 AU. Icarus 7, 779

[2] [VanderPlas J.T. (2018) Understanding the Lomb-Scargle Periodogram. The Astrophysical Journal Supplement 236, 1

[3] Hoffman T. et al. (2025) Debiasing astro-photometric observations with corrections using statistics (DePhOCUS). Icarus 426 116366.

ERDF project No. 1.1.1.5/2/24/A/004

Prospects and Problems of Microwave Observations of the Sun with RT-32 Radio Telescope

Dmitrijs Bezrukovs

Ventspils International Radio Astronomy Centre, Ventspils University of Applied Sciences, Latvia

e-mail: dmitrijs.bezrukovs@venta.lv

Microwave observations of the Sun and studies of solar microwave polarized emission is still a significant issue of the solar physics and one of scientific activities of Ventspils International Radio Astronomy Centre (VIRAC). The microwave polarized emission (1-10 cm) of the Sun is created in the upper chromosphere and the lover corona depending on frequencies. Studies of its spatial and spectral distribution provides the opportunity of direct localization emission's sources above the photosphere and direct measurements of plasma parameters and coronal magnetic field inductions in active regions.

Nowadays VIRAC implements routine microwave spectral polarimetric observations of the Sun with RT-32 radio telescope equipped by the new multichannel low noise spectral polarimeter LNSP4. The spectral polarimeter covers the frequency range 4.1-14.1 GHz (2.1-7.3 cm) divided to 12 frequency channels for right and left circular polarizations. The LNSP4 is integrated into the antenna drive control system and the data acquisition pipeline to provide automatic observations of the Sun, a storage of data into the multilevel archive and some primary processing of data.

The result of the routine observational session is a set simultaneous 2D maps of Stokes I and V parameters distribution over the disk of the Sun for a number of frequency bands. Some successful test observations for full per beam microwave flux monitoring of separate active regions with a high probability of solar flares were performed also.

Some feasible tasks of solar physics which could be based on these microwave observations of the Sun were distinguished as:

- Studies of radio brightness of the quiet Sun and coronal holes.
- Analysis of coronal hole-like areas associated with open magnetic fields which could be expected as sources of the slow solar wind
- Analysis of the microwave polarized emission of solar active regions for revealing of coronal magnetic fields based on the quasi-transverse emission's propagation
- Studies of microwave flux fluctuations resulting by magnetic field emergencies in active regions
- Analysis of quasi periodic pulsations (QPP) of the microwave flux as precursors of solar flares.

The presentation concerns to technical issues of solar microwave observations with VIRAC RT-32 radio telescope and shows some solutions of relevant solar physics tasks based on it.

Acknowledgments: The work is supported by “Multi-Wavelength Study of Quasi-Periodic Pulsations in Solar and Stellar Flares” (STEF), lzp-2022/1-0017 and “Novel proxies and approaches for solar flare forecasting”, lzp-2024/1-0023 (FLARE) projects.

ERDF project No. 1.1.1.5/2/24/A/004

Multi-harmonic and special shape/pattern/template approximations of discrete signals with generally irregular arguments

Ivan L. Andronov[1], Hanna M. Akopian[1], Vitalii V. Breus[1], Lidiia L. Chinarova[1], Larysa S. Kudashkina[1], Nina V. Savchuk[1], Serhii I. Iovchev[1], Vladyslava I. Marsakova[2,3], Serhii V. Kolesnikov[3], Maksym Yu. Pyatnytskyy[4]

[1]Dep. "Mathematics, Physics and Astronomy", Odesa National Maritime University, Ukraine
[2]Odesa Richelieu Science lyceum, Ukraine
[3]Main Astronomical Observatory, National Academy of Sciences, Ukraine
[4]Private Observatory "Osokorky", Ukraine

e-mail: tt_ari@ukr.net

"There is no sense to elaborate new methods for the time series analysis,
As even Ptolemy knew the Fourier Transform"
© The anonymous referee (1996

Introduction

The diversity of the types of deterministic and stochastic signals needs adequate methods for the statistically optimal data analysis. Real detected signals are never infinite and are discrete. Often there are large gaps between the observations, which drastically complicate power spectra, cross- (and auto-) correlation functions, functions of the parameters.

The paper, which got the referee report cited in the epigraph, was published in another (much more respectable) journal [1]. There are improved complete expressions which describe statistical properties in the complex case of "running" approximation merging separate algorithms:

- irregularly spaced discrete data
- an arbitrary covariation matrix w_kj of the statistical errors of the measurements, which extends the "diagonal" case of the "Gaussian weights"
- multiplicative "window" function p(z_k,z_j), like in the wavelets.

Despite each of these topics are discussed separately, also with special shapes, the algorithms of the joint improvements are more complicated and have been discussed in [1,2].

Algorithms

The generalized version of a scalar product of the two vectors $\vec{a}$ and $\vec{b}$, which is used for further analysis, may be expressed as

$$(\vec{a}\cdot\vec{b}) = \sum_{kj=1}^{n} p(z_k, z_j)\cdot w_{kj}\cdot a_k\cdot b_j, \quad (1)$$

here $z_j = (t_j - t_0)/\Delta t$, where t_j – as a j –th argument of the signal $t_j, x_j, j = 1..n$. In the "wavelet" terminology, t_0 is called "shift", and Δt – "scale". Often (but not exclusively), the weight function is symmetrical $p(\pm z_k, \pm z_j) = p(\pm z_j, \pm z_k) = p(\pm z_k)$, then t_0 is the center of the interval of the approximation, in which the data are placed generally asymmetrically.

The test function, may be generally written as:

$$\Phi(x_j; C_\alpha) = (\vec{x} - \vec{x}_C)^2 = \sum_{kj=1}^{n} p(z_k, z_j) \cdot w_{kj} \cdot (x_k - x_{Ck}) \cdot (x_j - x_{Cj}) \qquad (2)$$

Here x_{Cj} are "calculated" values at arguments t_j according to the approximating function $x_C(t, C_\alpha)$, where $(C_\alpha, \alpha = 1..m)$ are "parameters" or "coefficients" of the mathematical model. Similarly to the basic method of the Least Squares "LS" proposed by Karl Gauss before 1805, one has to determine the set of the parameters C_α, which minimizes the scalar function Φ. This corresponds to m "normal" equations $\partial\Phi/\partial C_\alpha = 0,\ \alpha = 1..m$. Generally, there may be a large number of solutions of these sets of the normal equations, which correspond to different values of Φ. This is typical for "non-linear" basic functions, in which the coefficients are involved inside, e.g, for the mono-periodic multi-harmonic approximation of order s

$$x_C(t) \quad = C_1 + \sum\nolimits_{j=1}^{s} (C_{2j} \cos(2\pi jft) + C_{2j+1} \sin(2\pi jft)) = C_1 + \sum\nolimits_{j=1}^{s} R_j \cdot \cos\left(2\pi jf\left(t - T_{0j}\right)\right).$$

The frequency $f = C_{2j+2}$ is also a parameter to be determined. In the periodogram analysis, the test function Φ is computed at a grid of equally spaced values of f with a recommended step $\Delta f = \Delta\varphi/sT$, where $\Delta\varphi \sim 0.05 \ll 1$, and T is duration of observations. The most popular our realization of the method is the software MCV [3,4], which also has a unique function to make a periodogram analysis taking into account a frequency-dependent trend, contrary to popular oversimplified detrending or pre-whitening.

For small number of parameters m, the approximation(=fit) may loose some systematic components of the signal. Such a situation is called "underfit", whereas large m correspond to an "overfit", where the approximation is better, following random fluctuations of the data (e.g. [5]). The statistically optimal number of parameters (of any approximation) is used practically:

- "Aesthetic" ="user-defined"
- ANOVA (=analysis of variances, Fischer's criterion, *p*-value, FAP=False Alarm Probability)
- Best statistical accuracy of the approximation (mean-squared or at extremum or any point).

The user-defined degree s is commonly used in many computer programs, including different electronic tables. The statistically optimal values using the ANOVA – type criteria are a next step of the analysis. E.g., the catalogues of the photometrical characteristics of long-period pulsating variable stars of different subtypes were published [6,7,8]. The atlas of the phase plane (x, x') curves was presented [9]. The sines and cosines may be combined into basic functions like (scaled and shifted) $\sin(\pi t)/(n \sin(\pi t/n))$.

The cubic polynomial splines were used also for the periodogram analysis and a search of the period changes [11]. The splines are more local and thus sometimes may have better approximations than the trigonometrical polynomial. However, the splines depend not on the number of basic points m, but also on the position (shift). Thus, there may be two improvements – either to find a best shift, or shift-averaged approximation. In this version, the data are still split into equal m subintervals, and the function of the interval is a cubic polynomial. In reality, the argument

t may be split into parts, e.g. maxima and quiescence for the outbursts, or eclipses in the binary stellar systems. The simplest "spline of changing order" (1;2;1) is an "asymptotic parabola" (AP) [12] This function consists of two inclined lines ("asymptotes") connected with a parabola, so the function and its derivative is continuous. This (generally asymmetric) approximation has $m = 5$ parameters, as well as a polynomial of 4-th order. However, AP seems to have smaller systematic deviations for the maxima of majority of pulsating variable stars. For AP, there are two "non-linear" parameters $q = 2$) – the positions of the borders between the parabola and the straight line. This approximation as good for the data in a logarithmic scale (e.f. brightness in stellar magnitudes), as the slopes of the lines may be used for computation of characteristic time scales of the ascending and descending branches of the light curve. This method was used in dozens of papers of our group. The comparison between this kind of spline $(q = 2)$, "symmetrical" polynomial $(q = 1)$ and ordinary algebraic polynomials $(q = 0)$ was presented by [13]. Generally, we use approximations with two "linear" parameters $\tilde{C}_1, \tilde{C}_2$, non-linear (shift C_3, scale C_4) and the rest describing the shape of the extremum [2]:

$$x_C[t] = \tilde{C}_1 + \tilde{C}_2 \cdot \tilde{G}\left((t - C_3), C_4, \dots, C_{mp}\right).$$

For non-logarithmic data, the (continuous with all derivatives) asymmetrical approximation for all the hump is $\tilde{G}\left((t - C_3), C_4, C_5\right) = \frac{2}{\exp\left(C_4 \cdot (t - C_3)\right) + \exp\left(-C_5 \cdot (t - C_3)\right)}$ [14]. This is an extension of the $\mathrm{sech}\,(z)$ popular symmetrical function. Even complicated function resembling the "log-normal" statistical distribution [15]:

$$\tilde{G}((t - C_3), C_4, C_5) = \exp\left(-\ln\ 2 \cdot C_5 \cdot (\ln\left(C_4 \cdot (t - C_3) + 1\right))^2\right)$$

This approximation is useless for nearly symmetrical signals because it does not converge.

These and other functions (totally, 22 of 11 types) have been involved in the software MAVKA [16] may be determined using order s g practical.

References

[1] Andronov I.L. (1997) Method of running parabolae: Spectral and statistical properties of the smoothing function. Astron. & Astrophys. Suppl., 125, 207-217 {1997A%26AS.125.207A}.

[2] Andronov, I.L. (2020). Advanced Time Series Analysis of Generally Irregularly Spaced Signals: Beyond the Oversimplified Methods, Knowledge Discovery in Big Data from Astronomy and Earth Observation. 191- 224. {2020kdbd.book.191A}

[3] [Andronov I.L., Baklanov A.V. (2004) Algorithm of the artificial comparison star for the CCD photometry. Astronomy School Report, 5, 264 –272. {2004AstSR.5.264A}

[4] Andronov I.L., Baklanov A.V. (2004) Multi-Column Viewer, MCV http://uavso.org.ua/mcv/MCV.zip

[5] Andronov I.L., Marsakova V.I. (2006) Variability of long-period pulsating stars. I. Methods for analyzing observations. Astrophysics 49 (3), 370-385 (2006Ap.49.370A)

[6] Kudashkina L.S., Andronov I.L. (1996) Fourier coefficients for the light curves of 62 Mira-type stars. Odessa Astronomical Publications, 9, 108-111. {1996OAP.9.108K}

[7] Marsakova V.I., Andronov I. L. Catalogue of Main Characteristics of Individual Pulsational Cycles of 18 Long-Periodic Stars. Odessa Astronomical Publications, 13, 83-176. {2000OAP. 13.83M}

[8] Chinarova L.L., Andronov I.L. (2000) Catalogue of Main Characteristics of Pulsations of 173 Semi-Regular Stars. Odessa Astronomical Publications, 13, 116-176. {2000OAP.13.116C}

[9] Kudashkina L.S., Andronov I.L. (2017) Phase Plane Analysis of the Photometrical Variations of Long-Period Variables. Odessa Astronomical Publications, 30, 93-97. {2017OAP.30.93K}

[10] Andronov I.L., et al. (2008) Idling magnetic white dwarf in the synchronizing polar BY Cam. The Noah-2 project. Central European Journal of Physics, 6, 385-401. {2008CEJPh.6.385A}

[11] Andronov I.L. (1987) Smoothing the" smoothing" cubic spline functions. Publications of the Astronomical Institute of the Czechoslovak Academy of Sciences. 70, 161 - 164 {1987PAICz.70.161A}

[12] Marsakova V. I.; Andronov I. L. (1996) Local Fits of Signals with Asymptotic Branches. Odessa Astron. Publ., 9, 127–130. {1996OAP.9.127M}

[13] Andrych K.D., et al. (2015) "Asymptotic Parabola" Fits for Smoothing Generally Asymmetric Light Curves. Odessa Astronomical Publications, 28, 158-160. {2015OAP.28.158A}

[14] Andronov I.L. (2005) Advanced Methods for Determination of Arguments of Characteristic Events. Proceedings of ASP Conference Series, 335, 37-53. {2005ASPC.335.37A}

[15] Bódi A., Szatmáry K., Kiss L.L. (2016) Periodicities of the RV Tauri-type pulsating star DF Cygni: A combination of Kepler data with ground-based observations. Astronomy & Astrophysics, 596, id.A24 {2016A&A...596A..24B}

[16] Andrych K.D., Andronov I.L., Chinarova L.L. (2020) MAVKA: Program of Statistically Optimal Determination of Phenomenological Parameters of Extrema. Parabolic Spline Algorithm and Analysis of Variability of The Semi-Regular Star Z UMa. Journal of Physical Studies, 24, 1902 {2020JPhSt.24.1902A}.

ERDF project No. 1.1.1.5/2/24/A/004

Experimental and First Principles Analysis of Dielectric and Optical Properties of Magnesium Alloys

Ashish Kumar Singh[1], Anatolijs Sharakovskis[2], Reinis Ingantans[2], Meldra Kemere[2], Arnolds Ubelis[1]

[1]Institute of Atomic Physics and Spectroscopy, FST, University of Latvia, Latvia
[2]Institute of Solid-State Physics, University of Latvia, Latvia

e-mail: kumar24@lu.lv

Introduction

Additive manufacturing processes are revolutionary in their flexibility and capability to manufacture complex shapes and parts without the need for assembly. Topologically optimized parts can only be economically manufactured, and in a timely manner, by additive manufacturing processes. One of the most useful methods for metal processing is Selective Laser Melting (SLM), which is a type of powder bed fusion additive manufacturing method where a metal powder bed is selectively melted with a laser to form apart from a 3D model in a layer-by-layer manner. Another is Laser Directed Energy Deposition, which uses laser to melt and deposit material from powdered or wire feedstock. Common lasers operate on electromagnetic radiation spectrum spanning the ultraviolet, visible and near infrared ranges denoted by '*UV-VIS-NIR*'. Each metal has different response to interaction with lasers due to their fundamentally different atomic structures, and the response varies as a function of the laser wavelength. For performing laser metal processing, the electromagnetic energy of the laser light needs to be transformed into thermal energy inside the metal, which is determined by the light absorption mechanisms in the metal. It is this absorbed energy, rather than the laser beam itself, that is available for heating the metal.

The purpose of this work is to investigate the optical-material relationships between lasers and magnesium (Mg) alloys. The work is focussed on developing a theoretical and practical understanding of the fundamental absorption and reflection mechanism of lasers with Mg alloys by obtaining spectral absorbance data for Mg alloy feedstock in different shapes and to obtain relationship between optical absorbance and laser beam characteristics. This will help in addressing some important issues that are faced by Mg alloys. Firstly, Mg alloys are reportedly difficult to process with lasers due to high reflectivity and the shortage of basic knowledge, and foundational understanding of their optical-material interactions. Secondly, laser additive manufacturing of Mg alloys has lagged all other structural and/or functional materials due to this problem. And thirdly, there is a significant lack of scientific results and experimental data pertaining to this subject, while copious amounts exist for other metals and alloys.

Materials and Methods

The research consists of a total of 3 materials: commercially pure AZ31, AZ80, and ZK60 alloys. These alloys are the most popular for use in various structural applications. The properties for pure metal are expected to be different from alloys due to the inclusion of alloying elements, as seen in Al alloys and steels [3]. Pure metal is used as a reference for other materials in obtaining the variation in absorbance due to alloying with various elements. A wide selection of materials will be useful to accurately create a property map between absorbance and chemical composition and adequately extract the overall optical behaviour of engineering materials with lasers of varying wavelengths. This information will be extremely important for engineering the Mg alloys for SLM.

The materials were procured in two (2) different forms, bulk shape, and powder feedstock. Bulk material, in the form of sheets & billets was procured from SME Engineering SIA (Riga, Latvia) and powders *(d: 20 -110 μm)* were supplied by Nanographi İnovasyon (Ankara, Turkey). Powders of pure Mg and AZ31 were also produced during a visit at Amazement Pvt. Ltd. (Warsaw, Poland)/ Prior to optical characterization, the surface was be characterized for quality, chemical composition, and roughness using scanning electron microscopy (SEM), energy dispersive X-ray spectroscopy, and surface profilometry. The materials were tested for their physical properties to understand their effect on the absorbance spectrum. It is well known that morphology of the incident surface affects the absorbance behaviour [1].

The metallography and sample preparation were performed on Buehler AutoMet 250 Pro at the Institute of Solid-State Physics, University of Latvia. The samples of size 15×15×7 mm^3 were embedded in epoxy resin molds of cylindrical shapes that are mounted on the polishing machine. The samples were subjected to grinding with 320, 400, 600, and 1200 grit SiC sanding papers until flat. After each step, the samples were cleaned ultrasonically in acetone bath for 60 seconds. After that, oil-based diamond suspensions of sizes 6, 3, and 1 μm were used to polish the samples. The polishing stage was set at 200 rpm and the sample holding head was set at 1.5 N load. Finally, the sample was polished with 0.05 μm colloidal silica suspension.

Optical properties and spectral absorbance of the materials was characterized using UV-VIS-NIR Spectroscopy on Agilent - Cary 7000 Spectrophotometer, and Reflection Electron Energy Loss Spectroscopy was performed on TF-ESCALAB Xi electron spectrometer. Ab-initio calculation using density functional theory (DFT) was performed on DFT package Quantum Espresso [2].

Results

The results of reflectivity measurement using photospectrometry are shown in Figure 1. As can be seen, the reflectivity of the alloys varies slightly in the 500 – 2000 nm wavelength range but drop sharply below 500 nm. This is an indication that the absorptivity of all the alloys increases for incident laser or light below 500 nm wavelength. The conventionally used IR laser of wavelength 1050 nm is indicated in the plot as well. For these alloys, a reduction of 10 – 20 % in the reflectivity can be observed at 400 – 500 nm compared to 1050 nm.

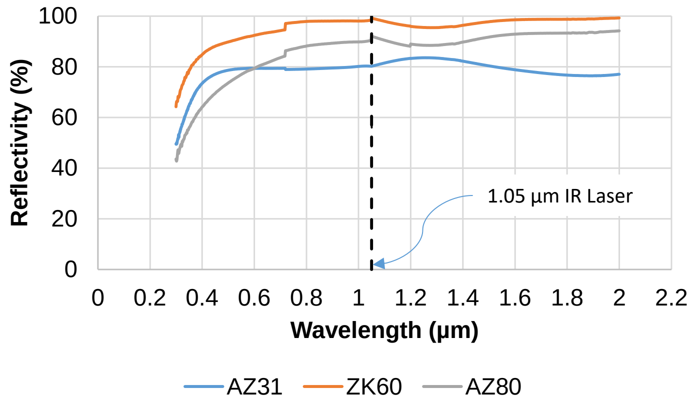

***Figure 1**. Reflectivity of polished surface as a function of wavelength of various alloys*

Reflected electron energy loss spectroscopy [3, 4] or REELS is a powerful tool for studying the properties of material at few nanometres depth from the surface. It is used to measure band structure and dielectric properties of the material. REELS was performed on polished AZ31 sample at 95 eV beam energy and the obtained spectrum is shown in Figure 2. The spectrum is processed using Richardson-Lucy deconvolution to deal with elastic interactions and the energy loss function (ELF) can be obtained. Then, the optical and dielectric properties of the material can be obtained.

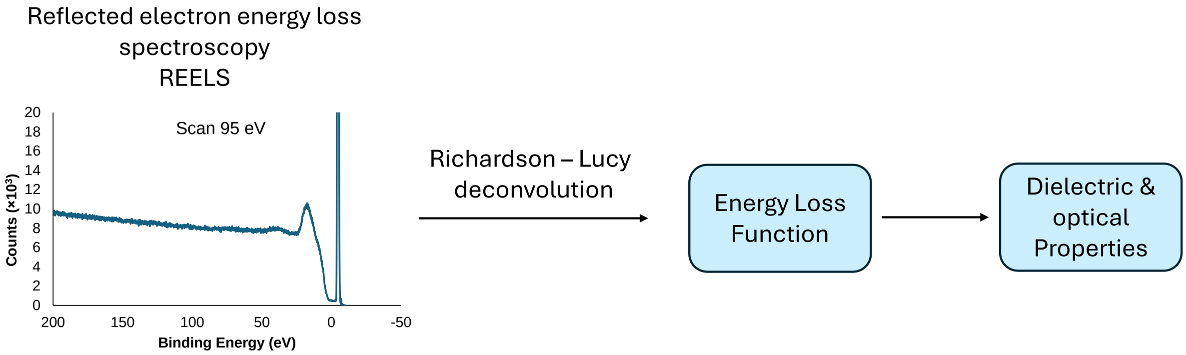

***Figure 2**. REELS spectra for AZ31 alloy and the methodology for extracting dielectric and optical properties of the material*

A supercell of 3x3x1 was used for the DFT simulation of pure Mg lattice. The supercell contained 72 atoms in HCP structure lattice, 50 k-point were used in the Brillouin Zone, and converged value of 120 bands were used in the calculation of the self-consistent field. The preliminary results are shown below in Figure 3.

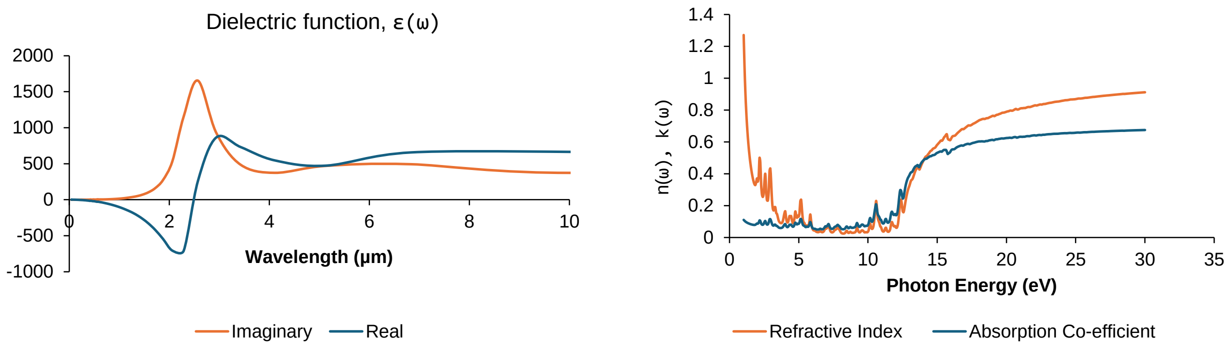

***Figure 3**. Results of DFT simulation showing (left) the complex dielectric function and (right) the refractive index and absorption coefficients for pure Mg*

Acknowledgments: This research was carried out as Postdoctoral Research work funded by Horizon Europe Research Executive Agency under the EU Marie-Sklodowska Curie Actions Grant No. 101153119.

References

[1] Niu, C., Zhu, T., and Lv, Y. (2019) Influence of Surface Morphology on Absorptivity of Light-Absorbing Materials. International Journal of Photoenergy, 2019: 1476217.

[2] Giannozzi, P., Baroni, S., Bonini, N., Calandra, M., Car, R., Cavazzoni, C., Ceresoli, D., Chiarotti, G.L., Cococcioni, M., Dabo, I., Dal Corso, A., de Gironcoli, S., Fabris, S., Fratesi, G., Gebauer, R., Gerstmann, U., Gougoussis, C., Kokalj, A., Lazzeri, M., Martin-Samos, L., Marzari, N., Mauri, F., Mazzarello, R., Paolini, S., Pasquarello, A., Paulatto, L., Sbraccia, C., Scandolo, S., Sclauzero, G., Seitsonen, A.P., Smogunov, A., Umari, P., and Wentzcovitch, R.M. (2009) QUANTUM ESPRESSO: a modular and open-

source software project for quantum simulations of materials. Journal of Physics: Condensed Matter, 21(39): 395502.

[3] Werner, W.S.M., Glantschnig, K., and Ambrosch-Draxl, C. (2009) Optical Constants and Inelastic Electron-Scattering Data for 17 Elemental Metals. Journal of Physical and Chemical Reference Data, 38(4): 1013-1092.

[4] Deris, J. and Hajati, S. (2017) Reflection electron energy loss spectroscopy as efficient technique for the determination of optical properties of polystyrene intermixed with gold nanoparticles. Applied Surface Science, 392: 697-70.

Experimentally induced darkening of dunite, a small step in understanding more about asteroid interlopers

Juulia-Gabrielle Moreau

Department of Geology, University of Tartu, Estonia

e-mail: juulia.moreau@ut.ee

In the classification of Main Belt asteroids [1], two recognized major asteroid types are the S-type and C-type asteroids. These asteroids possess very different reflectance spectra, which, in the near-infrared, show silicate (olivine/pyroxene) absorption bands for the S-type asteroids and are devoid of these absorption bands for the C-type asteroids. It has been studied that some of these C-type asteroids might be asteroids of the S-type [2, and reference therein] owing to the loss of silicate absorption bands from the darkening of the asteroid material. One major cause for the darkening is the so-called shock-darkening, where iron sulphides and metals melt and migrate between silicate fractures and grain boundaries [2]. Considering that these spectral changes are crucial in correctly classifying asteroids, their extent is yet to be thoroughly investigated. Recent research [3] has tried to understand one of the leading causes of shock-darkening. A dunite cube was doped with troilite (FeS) and placed in a high-temperature furnace. The whole dunite bulk was consequently darkened, which suggests breccia emplacement in a melt of asteroid fragments during asteroid collisions. Although the research needs a profound understanding of the spectral changes, it still marks an essential step in understanding how asteroids can be misclassified from S-type to C-type asteroids.

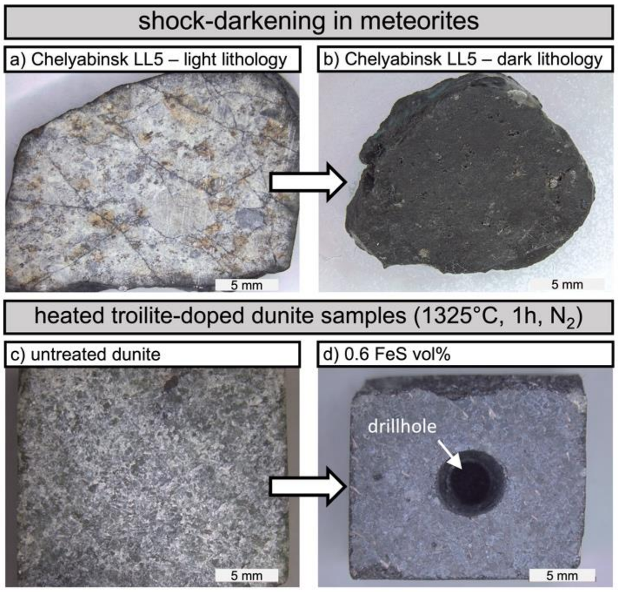

Figure 1. *Induced darkening in a dunite fragment by adding troilite (FeS) into a drillhole*

Acknowledgments: financial support of the ERDF Mobilitas Pluss programme, Estonia (MOBJD639).

References

[1] DeMeo F. E. et al. (2009) Extension of the Bus asteroid taxonomy into the near-infrared. Icarus 202: 160–180

ERDF project No. 1.1.1.5/2/24/A/004

[2] Kohout T. et al. (2014) Mineralogy, reflectance spectra, and physical properties of the Chelyabinsk LL5 chondrite - Insight into shock-induced changes in asteroid regoliths. Icarus 228: 78–85

[3] Moreau et al. (2024) Experimentally induced troilite melt pervasion in chondritic analogue materials: a study for FeNi-FeS darkening in chondrites. Meteoritics & Planetary Science, 59(12), 3229-3249.

Plasma emission spectroscopy and its role in the study of the heavy elements

Maria Teresa Belmonte, Pratyush Ranjan Sen Sarma, Santiago Mar

Department of Theoretical, Atomic Physics and Optics, University of Valladolid, Spain

e-mail: mariateresa.belmonte@uva.es

The spectroscopic analysis of the radiation emitted by different light sources is a powerful tool for the study of the atomic structure and the measurement of atomic parameters. Such parameters include, but are not limited to, wavelengths, energy levels, transition probabilities (Einstein coefficients for spontaneous emission), hyperfine structure constants and isotope structure. The knowledge of these parameters is essential in many fields for the interpretation of different phenomena. In the field of astrophysics, the analysis of stellar chemical abundances or the study of kilonova spectra relies on the availability of atomic data for the identification of the various elements present in the spectra recorded by different galactic surveys. However, despite their importance, experimental data for heavy elements remains scarce, especially for singly and doubly ionised species, due to their spectral complexity and the technical challenges associated with producing and diagnosing suitable plasmas.

The Atomic Spectroscopic Laboratory at the University of Valladolid has more than 40 years of experience in the measurement of atomic parameters of neutral, singly and doubly ionised elements using emission spectroscopy. We have performed studies of Stark widths and shifts and measured transition probabilities of a wide range of elements, including He, Ne, Ar, Kr, Xe and more recently heavy elements such as Nd.

The experimental setup

We have two different types of discharge sources available in our laboratory. The first is a pulsed-discharge lamp, which is used for the study of spectra of noble gases at pressures of approximately 200 Pa, employing voltages of up to 8 KV [1]. This lamp has been designed to obtain a good approximation to the partial local thermodynamic equilibrium so that the population of the energy levels of the atoms under study can be approximated to the Boltzmann distribution. The plasma produced in this lamp lasts for 200 µs. The configuration of the apparatus enables the acquisition of spectra at various temporal points following the discharge, ranging from 50 µs to 120 µs. The lamp is positioned within the arms of a Michelson interferometer, which allows for the measurement of the electron density evolution during the plasma's lifetime. At the pressures and electron densities employed in this lamp, the primary broadening mechanism of the spectral lines emitted by the plasma is Stark broadening (Lorentzian profile).

A second type of light source has recently been incorporated for the measurement of spectra of heavy elements [2]. This is a custom-built hollow cathode lamp, modelled on the design of the one used at the Fourier Transform Spectroscopy group at Imperial College London. This lamp uses a cathode composed of the element under investigation (neodymium at present) and features a carrier gas that is flowed at a pressure calibrated to ensure a stable discharge and an optimal signal-to-noise ratio for the spectral lines of interest. The selection of the carrier gas is key in facilitating the population of the energy levels that are the subject of our study. This lamp's primary broadening mechanism is attributed to Doppler broadening (Gaussian profile). The lamp is water-cooled to reduce this broadening as far as possible and to protect the cathode from melting due to the high temperatures it reaches.

To analyse the radiation emitted by our light sources, we use a 1.5 Jobin-Yvon monochromator with a Czerny-Turner configuration equipped with a UV optimised diffraction grating with 2400 lines/mm. This gives as a resolving power of 140 000 at 400 nm. The width of the monochromator´s entrance slit is chosen to maximise the quantity of light, while ensuring that we do not lose resolving power. We have also a Fabry-Pérot interferometer with resolving power of up to 10^8.

Following the measurement of the spectrum and its irradiance calibration, the next step is to fit it to a mathematical model. This model incorporates a first- or second-degree polynomial for the background, as well as a sum of functions, either Gaussians, Lorentzians, or a convolution of the previous functions, depending on the predominant broadening mechanism present in the lamp. The calculation of the areas of the spectral lines, along with their respective uncertainties, is then performed utilising a bespoke program developed within our laboratory. This program is available for download from our laboratory's Zenodo repository [3]. A comprehensive mathematical exposition of the expressions utilised in this program can be found in [1].

In this talk, we will give a comprehensive overview of the capabilities and limitations of our experimental setup. The final aim of this contribution is to foster collaboration with other groups working on atomic spectroscopy and with data users in need of new measurements.

Acknowledgments: This work was conducted under the Spanish government through project PID2021-127786NA-100 funded by MICIU/AEI /10.13039/501100011033 and by FEDER, UE. M. T. Belmonte acknowledges the Beatriz Galindo Fellowship from the Ministerio de Ciencia, Innovación y Universidades of the Spanish Government. P. S. Sen Sarma thanks the University of Valladolid for his Ph.D. grant.

References

[1] Belmonte M.T., Mar S., Djurović S., Menéndez J.A., Gavanski L. (2025) Experimental Transition Probabilities and Oscillator Strengths of Singly Ionised Xenon (Xe II) in the Ultraviolet: A Fully Statistical Approach to the Determination of Uncertainties. *Spectrochimica Acta Part B: Atomic Spectroscopy* 202, 107190. https://doi.org/10.1016/j.sab.2025.107190

[2] Sen Sarma, P.R., Belmonte, M.T. and Mar, S. (2024). Characterisation of a hollow-cathode lamp to measure accurate branching fractions of rare-earth elements. The European Physical Journal D, 78(6), p.76

[3] Mar S. (2024) Atomic transition probabilities with uncertainties. Zenodo. https://doi.org/10.5281/zenodo.13173712.

ERDF project No. 1.1.1.5/2/24/A/004

Quantum and nonlinear plasmonics on crystalline gold surfaces

Sergejs Boroviks

Nanophotonics and Metrology Laboratory, École Polytechnique Fédérale de Lausanne, Switzerland

e-mail: sergejs.boroviks@epfl.ch

Plasmonics offers unique ways to concentrate and manipulate light in regions of space much smaller than the diffraction limit [1]. Yet, the description based on the classical electromagnetism is valid even for deeply subwavelength plasmonic nanostructures. However, when the nanostructure dimensions approach mesoscopic regime, quantum confinement becomes appreciable, breaking the classical model. For example, this manifests in appearance of the so-called nonlocal response in ultrathin metal-insulator-metal waveguides, resulting in the distortion of the dispersion relation of gap surface plasmon modes [2], as illustrated in Fig. 1.

In this talk, I will discuss recent experimental advances in the field of quantum plasmonics and show why exceptional optical properties of monocrystalline gold flakes [3] are of paramount importance for characterization of these mesoscopic effects. Atomically smooth surfaces and well-defined morphology make such crystals excellent "sandbox" model for experimental studies of electron dynamics. Furthermore, {111}-type surfaces of such monocrystalline samples exhibit unusual second- and third-order nonlinear optical response [4-6], which is not observable with conventional, polycrystalline gold thin-films.

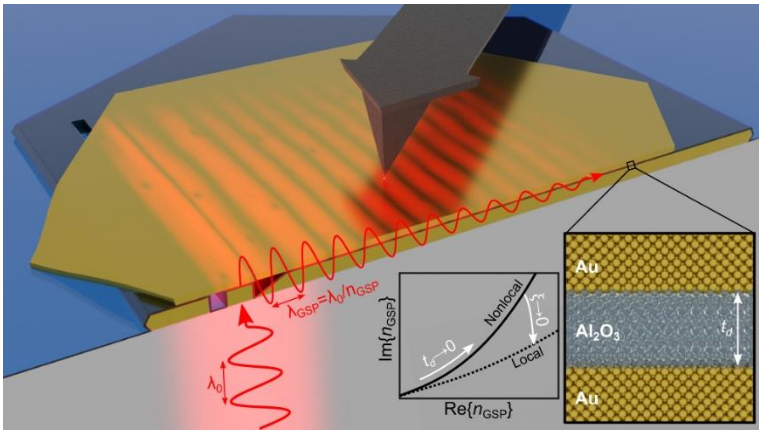

Figure 1. *Schematic illustration of the scanning near-field microscopy experiment probing nonlocal response in metal-insulator-metal heterostructure that ultraconfined gap surface plasmon modes. Reprinted with permission from ref. [2].*

References

[1] Gramotnev D., et al, (2010) Plasmonics beyond the diffraction limit. Nature Photonics 4, 83

[2] Boroviks S., et al. (2022) Extremely confined gap plasmon modes: when nonlocality matters. Nature communications 13, 3105

[3] Leibsir Y., et al. (2022) Ultimate Limit for Optical Losses in Gold, Revealed by Quantitative Near-Field Microscopy. Nano Letters 22, 5759

[4] Boroviks S., et al., (2021) Anisotropic second-harmonic generation from monocrystalline gold flakes. Optics Letters 46, 833

[5] Echarri A., et al., (2023) Nonlinear Photoluminescence in Gold Thin Films. ACS Photonics 10, 2918

[6] Boroviks S., et al., (2025) Monocrystalline Gold Metasurface to Control Anisotropic Second-Harmonic Generation. Advanced Optical Materials 2402525.

ERDF project No. 1.1.1.5/2/24/A/004

Coherent manipulation of quantum states using the Autler-Townes effect

Artūrs Ciniņš

Institute of Atomic Physics and Spectroscopy, FST, University of Latvia, Latvia

e-mail: arturs.cinins@lu.lv

I will report on the scientific results of my PhD dissertation work. The research focuses on achieving high-fidelity coherent control of quantum states in multilevel atomic systems using the Autler-Townes effect [1]. In contrast to model few-level systems, where various coherent control schemes can be implemented with relative ease, multi-photon excitation schemes in real atoms often involve multiple non-degenerate sublevels. For example, fine structure levels of many atoms exhibit hyperfine structure. The hyperfine interaction scales as 1/n3 and is usually negligible for highly excited states, therefore individual addressing of hyperfine sublevels is restricted to low-lying excited states at low laser coupling strength. Adiabatic coherent control methods, on the other hand, require strong laser couplings to avoid losses. Efficient coherent population transfer between the ground state and Rydberg states then inevitably involves multiple excitation pathways, and their mutual interference can lead to very complicated excitation dynamics.

Hyperfine splitting of alkali metal atom ground state can span several GHz, while already in the first excited state it reaches only tens to a few hundred MHz. When the laser coupling strength reaches hundreds of MHz, one can only address individual hyperfine components in the ground level. Excitation of two hyperfine ground level components via an intermediate manifold to a Rydberg state resembles a tripod excitation scheme, where three (meta)stable levels are all coupled to a single fast decaying level. Total or partial adiabatic population transfer between the stable levels can be performed with high fidelity [2].

Decomposition of two-photon excitation schemes in alkali metal atoms into bright and dark states using the Morris-Shore transform [3] reveals intricate interplay between coherent laser coupling and intra-atomic hyperfine interactions. The perturbation introduced by the hyperfine interaction leads to the observation of “chameleon” states — states that change their appearance in the Autler-Townes spectrum, behaving as bright states at small to moderate coupling, and fading from the spectrum similarly to dark states when laser coupling strength exceeds the hyperfine mixing in the excited manifolds [4]. The chameleon states can be further classified as “slow” or “fast”, depending on their divergence rate relative to the bright components of the Autler-Townes spectrum [5].

Analysis of bright and dark states formation in two-photon excitation schemes in alkalis has revealed orthogonal excitation pathways, each coupled to a different hyperfine component of the ground state. While the hyperfine interaction mixes the two pathways, this mixing can be disrupted by introducing a specifically tuned control laser, which couples the intermediate excitation manifold to an unpopulated level. Application of the control laser allows $\Delta F \equiv 0$ excitation with fidelity exceeding 99.99% [6].

Acknowledgments: This research was partially supported by Latvian Council of Science project No. lzp-2019/1-0280 and by Latvian Council of Science project No. lzp-2023/1-0199.

References

[1] S. H. Autler and C. H. Townes, Phys. Rev. 100, 703, doi.org/10.1103/PhysRev.100.703 (1955)

[2] A.Cinins, M.Bruvelis, N.N.Bezuglov, J. Phys. B: At. Mol. Opt. Phys. 55 234003, doi.org/10.1088/1361-6455/ac9a90 (2022)

[3] J. R. Morris and B. W. Shore, Phys. Rev. A 27, 906, doi.org/10.1103/PhysRevA.27.906 (1983)

[4] T.Kirova, A.Cinins, D.K.Efimov, M.Bruvelis, K.Miculis, N.N.Bezuglov, M.Auzinsh, I.I.Ryabtsev, A.Ekers, Phys. Rev. A 96, 043421, doi.org/10.1103/PhysRevA.96.043421 (2017)

[5] A.Cinins, M.Bruvelis, M.S.Dimitrijević, V.A.Srećković, D.K.Efimov, K.Miculis, N.N.Bezuglov, A.Ekers, Astron. Nachr., 343, e210081, doi.org/10.1002/asna.20210081 (2022)

[6] A.Cinins, D.K.Efimov, M.Bruvelis, K.Miculis, T.Kirova, N.N.Bezuglov, I.I.Ryabtsev, M.Auzinsh, A.Ekers, Phys. Rev. A 109, 063116, doi.org/10.1103/PhysRevA.109.063116 (2024).

ERDF project No. 1.1.1.5/2/24/A/004

Application of resonance atomic spectra lines of Se I and Te I in measurement transmittance of optical fibers in far UV

Aleksandrs Koļesņiks, Arnolds Ūbelis, Austris Pumpurs

NSP FOTONIKA-LV, Latvia

e-mail: aleksandrskolesniks45@gmail.com

Introduction

This research investigates the application of Selenium and Tellurium atomic spectral lines to evaluate the transmittance of high-quality optical fibers in the far ultraviolet region, specifically below 200 nm. Due to commercially available solutions, using Deuterium lamps that nearly cut off at 200nm [1], this method using atomic spectral lines offers a practical solution.

Methods

Our team used Se and Te electrodeless low-pressure lamp that were powered by an RF-ICP generator, producing intensive resonance spectra of Se I and Te I [2],[3]. Two experimental systems were created, both using Princeton instruments SpectraPro 2300 monochromator and 1200 line grating. One of these systems used 5 meters long optical fiber, while the other one used a quartz tube filled with weak nitrogen flow to eliminate atmospheric oxygen's absorption of UV spectrum, allowing us to detect spectra under 180nm.

Results

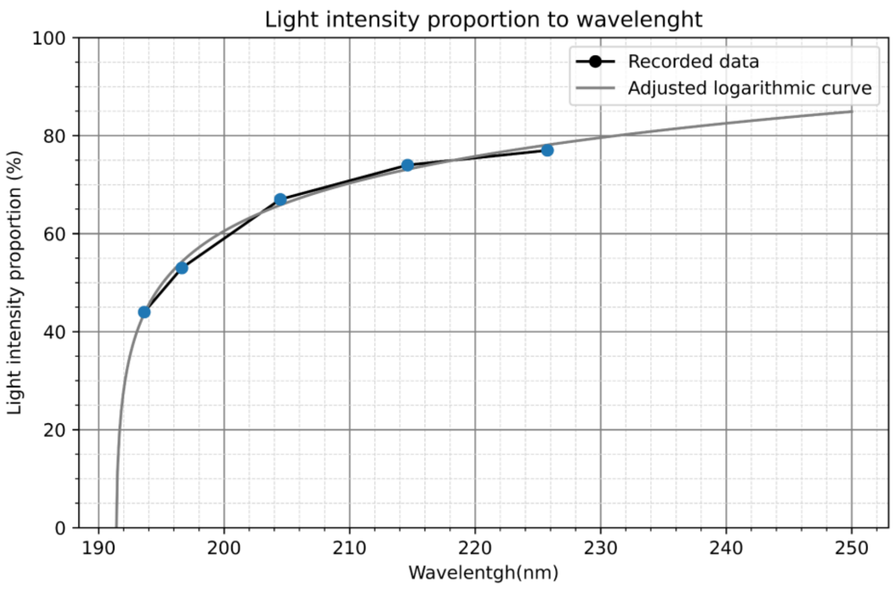

Figure 1. *Light transmittance depending on wavelength, with a logarithmic curve to predict transmittance in different wavelengths*

The results show intense Se I, Te I spectra lines, such as Se I at 196.09nm and 203.98 nm, and Te I at 214.72nm and 226.55nm, as well as one C I line at 193.09nm [4]. Comparison of two detection methods acquired data reveals reduced transmittance at shorter wavelengths. A logarithmic graph was used as a model to visualize the relation between transmittance and wavelength. In the results, used optical fiber showed relatively high transmittance till 200nm with a steep decline till 190nm (Fig. 1.)

Conclusions

This method of measuring transmittance is efficient, cost-effective and suitable for applications both in research and industry. There is a potential to expand this method by combining other elements in lamps, such as As and Sb.

References

[1] https://www.flickr.com/photos/bob_81667/35443318076/in/photostream/

[2] Ubelis, A. P., Berzinsh, U. V. (1986). Transition probability measurements of Se I spectral lines by emission method. Physica Scripta, 1986, 34 (6B), S. 805-806

[3] Ubelis, A. P., & Berzinsh, U. V. (1983). Transition probability measurements of Te I spectral lines by methods of emission and absorption of radiation. Physica Scripta, 28(2), 171-178

[4] https://physics.nist.gov/PhysRefData/ASD/lines_form.html.

ERDF project No. 1.1.1.5/2/24/A/004

Dirac Delta pulse generator – powerful tool for diagnostics in electronics

Arman Bzhishkian, Jānis Blahins

Institute of Atomic Physics and Spectroscopy and *NSP FOTONIKA-LV, University of Latvia*

e-mail: janis_59@inbox.lv

A single spike pulse function e^(ikx) or Dirac delta function is convenient for diagnostics because its Fourier transform in time axes is 2πδ(k) or a flat, monotonic, constant wave function. Although such an idealized spike pulse function cannot be obtained by electronic methods, its equally effective narrow bell-shaped function can be easily obtained, which is handy tool for practical work, as long as the pulse width is significantly narrower than the time constant (respectively, the reciprocal passband) of the semi-resonant medium under study. Sending the next pulse before at least 20 pulse widths have passed is undesirable. The most important thing is to achieve such a Delta pulse "train" (pulse train) or pulse comb (Dirac comb), because its transformation on the time scale is an infinite horizontal band from zero to infinity [1]. That is, the system under test (DUT = device under test) receives all possible frequencies simultaneously in one short action and refers to those in which it can resonate. Thus, with one short action, the full frequency characteristic curve of the DUT can be recorded.

How to implement it practically? Back in the eighties, it seemed that the fastest pulse could be obtained from two logic elements, one of which is powered by the other, so only a needle created by the transition process of the logic elements runs through. By slightly extending it with the help of an RC circuit, debouncing buttons were built at that time. However, the maximum operating frequency of the USSR 155/133 series chips did not reach 100 MHz, and even the 500/100 series did not reach 1 GHz. In this regard, the theory and even the element base for avalanche transistors are well developed today, and in avalanche mode it is able to achieve a pulse several orders of magnitude shorter than one might think from semiconductor passband data. In avalanche mode, the transistor is orders of magnitude faster than f(T). The Edaboard electronics discussion forum [2] recommends a scheme. If the FMMT413TD transistor is used, then a supply voltage of about 100 V is required to induce the avalanche mode, and the resulting needle has a length of approximately 0.35 nanoseconds and an amplitude of about 2 kV, which is more than enough for all kinds of tests: for determining VSWR in antennas, for measuring the length or wave shortening factor in antenna cables, for determining the location of a transmission line break, for finding a coil break (reflects a positive pulse) or a short circuit (reflects an inverted pulse), for measuring the gain factor, for measuring the passband of a probe, for EMI immunity tests udc [3]. This specialized avalanche transistor is quite hard to find, and there are also ones that are less than 100 times cheaper than the 2N2369A, which I tried and managed to get 2 ns spikes at 80 V and 2N3904 at 180 V for about 1.7 ns. Even with the BC337-25 or the BC548B, you can get pulses of about 7 ns or shorter, which can be almost sufficient in many cases. The resistance value and capacitor capacitance depend on the transistor: for the 2N2369A, 10K and 27 p to 33 p or 1M and 4p7; for the BC337 and BC548, 4k7; for the FMMT413, 4k7 to 10K and 200 p. To some extent, such transistors as 2N2222, 2N4441, MPSA44, BC107, BC337, S9014, S8050, etc. can also be forced to enter the avalanche mode. For very short pulses, it should be noted that BNC connectors paired with RG58 cannot work above 4 GHz, but SMA with RG405 can work up to 12 GHz.

There are at least several publications with corresponding circuits: [4] have created a rather complicated solution using a multi-stage FMMT417, which reaches 300 V and 0.7 ns. [5] recommends 2N3904. With 2SC5773, in [6] it was possible to obtain a rise time of 0.7 ns and a decay time of 1.3 ns. A fairly high-level study can also be found in [7] with a photopulse output to a fiber, which can be very useful for research in the field of photonics. To obtain the avalanche-causing high voltage, any design of power supply circuit can be used, even if it is as clumsy as [8], but the most common are direct conversion with a multi-winding block generator [9], which with a 2N3904 reaches 1.7 ns and 200 V, or with the help of a Step-Up chip [10] and its LT-Spice computer simulation [11], for example, the LT1073, which can operate even from a single finger battery, with a 2N2369 reaching 0.35 ns and 90 V. The circuit [12] is also very similar. In [13] this circuit is supplemented and even the printed circuit board topology can be found. A lot of good theoretical insights and practical information about this design can be found in [14], although reaching only 7 ns.

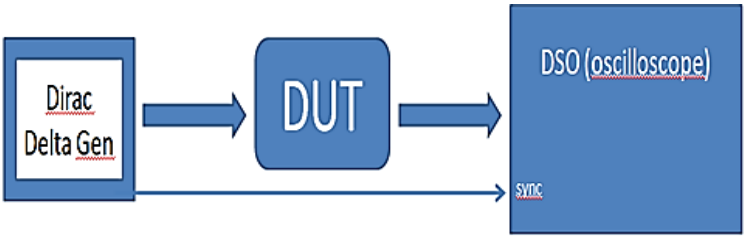

Figure 1. *Typical Delta generator circuit*

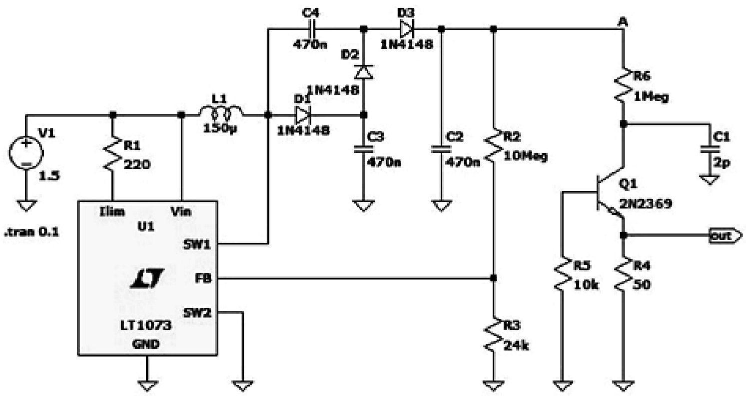

Figure 2. *Typical DUT connection to the test set and the obtained oscillograms on our soldered pcb.*

References (*all internet links last accessed on 01.03.2025*)

[1] https://dsp.stackexchange.com/questions/35475/what-is-the-fourier-transform-of-deltat-a

[2] https://www.edaboard.com/threads/avalanche-pulse-generator.402966

[3] Bas ten Have1, Tom Hartman1, Niek Moonen1, Frank Leferink (Sept.2019). Why Frequency Domain Tests Like IEC 61000-4-19 Are Not Valid; a Call for Time Domain Testing. Proc. of the 2019 International Symposium on Electromagnetic Compatibility. 10.1109/EMCEurope.2019.8872070

[4] Pavitra Krishnaswamy, Andras Kuthi, P. Thomas Vernier, Martin A. Gundersen (August 2007). Compact Subnanosecond Pulse Generator Using Avalanche Transistors for Cell Electroperturbation Studies. IEEE Transactions on Dielectrics and Electrical Insulation Vol. 14, No. 4, 857.pp;

[5] https://www.codrey.com/electronic-circuits/avalanche-pulse-generator-an-introduction/

[6] https://hackaday.io/project/169376-avalanche-breakdown-pulse-generator-tdr-g1/details

[7] Joan Canals, Nil Franch, Oscar Alonso, Anna Vilā, Angel Diéguez (Jan 2019). A Point-of-Care Device for Molecular Diagnosis Based on CMOS SPAD Detectors with Integrated Microfluidics. Sensors 19(3):pp 445, DOI:10.3390/s19030445

[8] https://hackaday.com/2016/10/04/a-quickly-hacked-together-avalanche-pulse-generator/

[9] https://tefatronix.g6.cz/display.php?page=avgen&lang=en

[10] https://electronics.stackexchange.com/questions/638895/simulating-an-avalanche-pulse-generator-in-ltspice

[12] https://entangledwaves.wordpress.com/2013/07/15/avalanche-pulse-generator/

[13] https://hackaday.io/project/169376-avalanche-breakdown-pulse-generator-tdr-g1/details

[14] LT Application Note AN-72. www.analog.com/media/en/technical-documentation/application-notes/an72f.pdf.

ERDF project No. 1.1.1.5/2/24/A/004

Measurement of atomic and ionized (B I and B II) spectra of hardly volatile Boron using unique technique - hybrid plasma system

Arnolds Ūbelis[1], Austris Pumpurs[1], Jānis Kļaviņš[1], Arman Bzhishkian[1], Jevgenijs.Gabrusenoks[2]

[1]NSP FOTONIKA-LV, University of Latvia, Latvia,
[2]Institute of Solid State Physics, University of Latvia, Latvia

e-mail: arnolds@latnet.lv

The measurement and studies of resonance spectra of hardly volatile chemical elements like Boron (melting point 2076ºC, boiling point 3927ºC) is an experimental challenge caused by difficulties of atomization. Therefore, the knowledge base of basic properties of B I and B II is not rich at all. Currently, to respond to increasing demand from atomic physics and astrophysics especially, and various technology disciplines, like analytical spectroscopy and advancement of implantation technologies of Boron ions (B II) in high purity germanium crystals [1], the key material used for high energy radiation sensors, currently demands development of more handy and cost-effective apparatus [2]. Particularly, a determination of the solar photosphere boron abundance was studied and published in 1999 [3]. An article appeared in 1997 reporting on the measurement of B II 1362 Å resonance line by Goddard High Resolution Spectrograph of Hubble Space Telescope observing four B-type stars from the Orion association [4]. Growing number of Space telescopes and advances in ground-based telescopes means need for richer knowledge base on the spectroscopy on atoms and ions including hardly volatile elements.

The latest data on Boron spectroscopy were published in 2009 [5], in 2010 [6] and are collected in worldwide known database [7]. A critical compilation of energy levels and spectral lines of neutral boron was made in [8]. On overall, there are many theoretical studies, and one research based on high power hollow cathode technologies with current up to 3 A [9].

The report is highlighting the first results of application of hybrid plasma system: hollow cathode discharge combined with low pressure inductively coupled radiofrequency plasma (HC & RF-ICP) in studies of spectroscopy of atomic boron.

References

[1] Fair R.B. (1998). History of Some Early Developments in Ion-Implantation Technology Leading to Silicon Transistor Manufacturing. Proc.of the IEEE, 86(1), 111-137

[2] Blahins, J., & Ubelis, A. (2022, March). Towards Next-Generation Small-Size Boron Ion Implanting Apparatus. In Proceedings of the Latvian Academy of Sciences, 76(2), 198-203

[3] Katia Cunha & Verne v. Smith (1999) A Determination of the Solar Photospheric Boron Abundance. The Astrophysical Journal, 512: 1006È1013

[4] Katia Cunha, David Llambert, Michael Lemke, Douglas R Ges, and Lewis C. Roberts. (1997) A Boron Abundance of B Stars of the Orion Association. The Astrophysical Journal, 478:211È224

[5] Zhang Tian-yi, Zheng Neng-wu. (2009) Theoretical Study of Energy Levels and Transition probabilities of Boron Atom. Acta Physica Polonica A.m Vol. 116 (2), 141-153

[6] Fuhr, J.R., W. L. Wiese, W.L. (2010) Tables of Atomic Transition Probabilities for Beryllium and Boron. J. Phys. Chem. Ref. Data, 39 (1), 141-153

[7] Kramida, A. (2006). NIST Atomic Energy Levels and Spectra Bibliographic Database

[8] Odintzova G., A., Striganov A., R. (1979) The Spectrum and Energy Levels of the Neutral Atom of Boron (BI). Journal of Physical and Chemical Reference Data 8 (1), 63-67 (1979); https://doi.org/10.1063/1.555592 Published Online: 15 October 2009

[9] Kramida, A. E., & Ryabtsev, A. N. (2007). A critical compilation of energy levels and spectral lines of neutral boron. Physica Scripta, 76(5), 544-552.

ERDF project No. 1.1.1.5/2/24/A/004

Measurement of atomic and ionized (Pb I and Pb II) spectra of Lead hybrid plasma system

Arnolds Ubelis[1], Zane Mētra[1], Aleksandrs Kolesniks[1], Janis Rupkus[2]

[1]NSP FOTONIKA-LV, University of Latvia, Latvia,
[2]Riga Photonics Centre, Latvia

e-mail: metrazane@gmail.com

The report is highlighting the first results of application of hybrid plasma system: hollow cathode discharge combined with low pressure inductively coupled radiofrequency plasma (HC & RF-ICP) in studies of spectroscopy of atomic lead. The experimental measurements and analysis showed the potential of substantial increase of knowledge base on the spectroscopic properties of atomic Pb I and eventually for ion Pb II. Current advances in atomic physics envisage that the data on atomic spectroscopy of Pb I and Pb II need to be substantially enriched, to open new opportunities for the studies of basic properties of atoms and ions of lead. The limiting factor for that, until now, were insufficiently intensive sources of emission needed for such research in case of lead, having low volatility. Substantial progress in theoretical atomic physics and growing needs of astrophysics indicate that new experimental data on atomic spectroscopy of atomic (Pb I) and ionic (Pb II and more) will lead towards increased accuracy theoretical calculations and broader use in astrophysics. Additionally, there is growing need to improve sensitivity, and to make more user-friendly methods, used in detection of traces of lead containing pollutants in the environment. Possible breakthrough – application of resonance fluorescence, which could be effectively used in case of presence of intensive sources of basic resonance lines. The best evidence of that, is the case of mercury, for which sophisticated resonance florescence techniques where developed, and standardised during the last decades increasing the sensitivity substantially [1]. Our research aims to move toward similar results in the case of lead.

The presentation and extended abstract of the conference will report the results of this pilot experiment indicating very promising outcomes for follow up research and future applications of such hybrid source of resonance spectra of atomic and ionic lead:

- The possibility to produce intensive source of resonance lines of lead with profiles of lines without reabsorption which means ideal case for both version (absorption and resonance fluorescence) of analytical spectroscopy.
- The presence of large number of spectral lines in the spectrum will allow branching ratio studies for many groups of spectral lines similar to our studies in case of Se I, [2], Te I [3] and As I [4].
- The presence of spectral lines of Pb II in the spectra from hybrid plasma indicates on broad opportunities to study ion spectra of lead for the first time, using RF-ICP & HC plasma.

References

[1] Telliard, W. A., and M. Andersson. (2005). Method 245.7 Mercury in Water by Cold Vapor Atomic Fluorescence Spectrometry. US EPA Office of Science and Technology, 1-33

[2] Ubelis, A. P., Berzinsh, U. V. (1986). Transition probability measurements of Se I spectral lines by emission method. Physica Scripta, 1986, 34 (6B), S. 805-806

[3] Ubelis, A. P., & Berzinsh, U. V. (1983). Transition probability measurements of Te I spec-tral lines by methods of emission and absorption of radiation. Physica Scripta, 28(2), 171-178
[4] Berzins, U., Ubelis, A., & Bziskjans, A. (2021). Branching fraction measurements of arsenic 4p25s-4p3 transitions. Journal of Quant. Spectr. and Radiative Transfer, 276, 107943Zhang Tian-yi, Zheng Neng-wu. (2009) Theoretical Study of Energy Levels and Transition probabilities of Boron Atom. Acta Physica Polonica A.m Vol. 116 (2), 141-153.

ERDF project No. 1.1.1.5/2/24/A/004

Exploring optoplasmonic doped whispering gallery mode microspheres

Inga Brice[1], Arvids Sedulis[1,2], Janis Alnis[1,2]

[1]Institute of Atomic Physics and Spectroscopy, FST, University of Latvia, Latvia
[2]Institute of Photonics, Electronics and Telecommunications, Faculty of Computer Science, Information Technology and Energy, Riga Technical University, Latvia

e-mail: inga.brice@lu.lv

Whispering gallery mode (WGM) resonators are well suited for wide variety of potential applications: filters, passive resonators, sensors, lasers, optical frequency combs (OFC). Due to their high quality (Q) factors, light beams are confined and sustained inside the resonator with small reflection losses thus enhancing light-matter interaction. This allows to reach high sensitivity to any perturbations of the surrounding environment or generating nonlinear effects at relatively low powers. The material, geometry and surface of the WGM resonator can be tailored to enhance desirable optical properties.

Silica doped with erbium is widely used for optical amplification. When erbium ions incorporate into silica sharp and temperature-stable transitions at 1530-1570 nm can be generated [1]. Adding gold nanoparticles on the resonator surface lead to localized surface plasmon resonances that extend the evanescent field and further enhance the sensitivity [2] while being highly chemically and photostable. The possibilities to combine the material doping and adding optoplasmonic metal nanoparticles to create a hybrid active/passive system has not been widely explored.

Lasing of erbium doped microspheres

We have fabricated silica microspheres doped with erbium ions. When pumped with 1470-1500 nm source emitted at 1530-1560 nm at a threshold of 1.6 mW [3]. Optimal concentration of Er ions is vital for generation of lasing signal, as both too high and too low concentration of Er ions incorporated into silica microspheres will not generate any lasing signal. Lasing was also observed when gold nanoparticles were deposited on the surface of the doped microsphere (see Fig. 1).

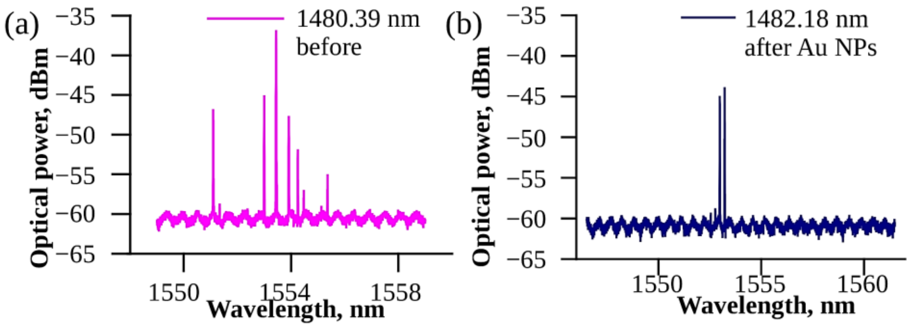

***Figure 1.** Lasing signal of Er-doped microsphere (a) before and (b) after additional deposition of gold nanoparticles*

Deposition of gold nanoparticles for optiplasmonics

Multiple depositions of gold nanoparticles using colloidal nanoparticles solution was performed. Comparing the case of no Au NPs (Fig. 2a) to each additional time sample is dipped into the Au

NPs (Fig. 2c-d), it can be seen that number of supported modes inside the microsphere decreases. Looking at transmission scan spectra, 3-5 dip-coating cycles into 1:10 diluted Au NP colloidal solution appear to have strong nonlinear broadening during red detuning Similarly, when observing the third harmonic green emission excited with CW 1550 nm laser for a sample doped with high concentration of erbium before (Fig. 2e) and after gold nanoparticle deposition (Fig. 2f-i), emission becomes more intense as Au NPs are added on the surface until disappearing completely after 4th dipping cycle. Further research into these hybrid doped optoplasmonic resonators is necessary with different types of dopants and plasmonic nanoparticles.

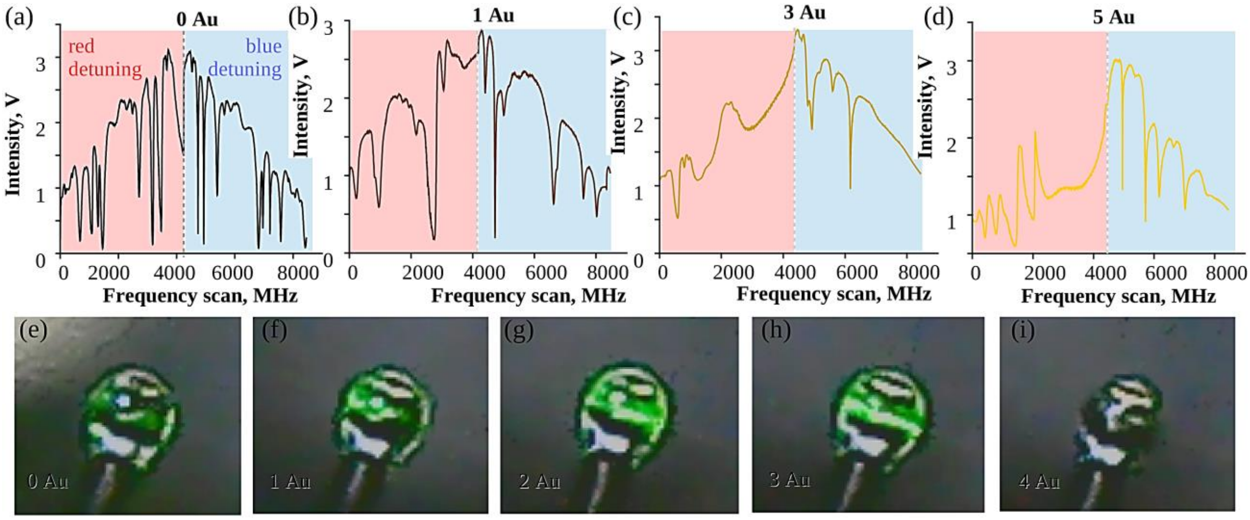

Figure 2. *Er doped microsphere sample for different number of dip-coating cycles into 1:10 Au NP solution (a)-(d) transmission spectra and (e)-(i) third harmonic generation*

Acknowledgments: The research is financed by the Recovery and Resilience Facility project "Internal and External Consolidation of the University of Latvia" (No.5.2.1.1.i.0/2/24/I/CFLA/007).

References

[1] Kalkman J., et al. (2006) Erbium-implanted silica microsphere laser. Nuclear Instruments and Methods in Physics Research Section B: Beam Interactions with Materials and Atoms, 242, 182–185

[2] A. Bozzola A, et al. (2017) Hybrid plasmonic–photonic whispering gallery mode resonators for sensing: a critical review. The Analyst, 142(6), 883–898

[3] Brice, I., et al. (2025) Tailoring whispering gallery mode resonator for a wide range of potential applications: optoplasmonic erbium doped microspheres. Journal of Physics: Conference Series 2978, 012004.

ERDF project No. 1.1.1.5/2/24/A/004

On current status of small sized innovative boron ion implantation apparatus

Jānis Blahins

Institute of Atomic Physics and Spectroscopy and *NSP FOTONIKA-LV, University of Latvia*

e-mail: janis_59@inbox.lv

4 years ago, FOTONIKA-LV won the ERDF competition for the development and testing of an innovative low-cost implantation device concept. Currently, the Project is completed and has received a 96% rating for scientific quality. The innovations of the device are based on the following technical solutions:

1. Since pure boron is a high-temperature material, but boron compounds are highly toxic, ions are obtained from pure boron, but with the help of a Hollow Cathode (HC) discharge, by gently heating boron to a temperature at which it rapidly loses its electrical insulator properties. Accordingly, HC allows obtaining a relatively large ion current without complex technical equipment.
2. Boron is filled into a cavity of purified carbon, which is a particularly convenient material that solves the problems of boron fixation on the walls.
3. Immediately behind the HC is a radiofrequency inductively coupled plasma (ICP) discharge coil, which provides a significant improvement in the ionization yield, behind which ions are extracted by the interaction of two mechanisms - a differential vacuum drop, which drives them towards the vacuum pump, and an electrostatic field created by a conical electrode. Behind the electrode is a stack of plate shaped electrodes, which allows focusing and minimal acceleration of the ion beam.
4. The vacuum system is made of quartz glass, which, firstly, is a material that is easy to manufacture or modify in laboratory conditions, and secondly, costs much less than the massive molybdenum metal vacuum recipient classically used in high-purity implantation apparatuses, and also provides, with a condition if surface degassing with ICP plasma is applied, slightly better vacuum purity than molybdenum and significantly better than stainless steel.
5. Further, instead of the usual technological double-focusing magnetic mass separator, the beam is cleaned of impurities by a quadrupole mass selector (QMS) radiofrequency mass separator, which we managed to order from the rod manufacturer for a relatively reasonable price, which guarantees such high manufacturing accuracy that beam losses in the mass filter are small.
6. The main accelerator is a linear multi-plate electrode system with a constant pitch, to which voltage is supplied through a resistive divider. It was found that for reasonably high exposure doses, a target wafer anti-charging system is not necessary. The target is, however, housed in a stainless-steel housing to prevent bremsstrahlung escaping into the environment, and the QMS circuit is also made of this metal to implement the grounding point.
7. All the Electronics around mentioned parts are made for occasion of our laboratory, using an original modern-day solutions like switched mode power supplies (SMPS), direct digital synthesis (DDS) generators, Cocroft-Walton circuit for 100 kV obtaining, devices-to-computer links etc.

8. Based on this work, a textbook was written in Latvian as part of the planned PhD Dissertation on ion technologies and technological equipment assemblies used in ion beam manipulation, their construction, calculations, alternatives and use. In total, 145 pages of text, 131 drawings, 9 tables, 127 formulas and 630 references were collected in it. Still is not yet quite clear how to publish this work if the images in it are the work of other authors, because there is no much experience in requesting the multiple author's permission. The dissertation is expected to be defended in the summer or early autumn of 2025.

ERDF project No. 1.1.1.5/2/24/A/004

Formation of LIPSS on GaAs in water using radially and azimuthally polarized laser beams

Kalvis Kalniņš[1], Uldis Bērziņš[1], Vyacheslav V. Kim[2], Rashid A. Ganeev[2]

[1]*Institute of Atomic Physics and Spectroscopy, FST, University of Latvia, Latvia*
[2]*Institute of Fundamental and Applied Research National Research University, Uzbekistan*

e-mail: kalvis.kalnins.lu@lu.lv

In this study, we demonstrate the fabrication of laser induced periodic surface structures (LIPSS) on gallium arsenide (GaAs) immersed in water. Ripples were inscribed in lines by moving the sample on the focal plane of the laser beam, which produced 532 nm, 30 ps pulses. An S-waveplate was used to convert the initially linearly polarized Gaussian beam into helical beam with either radial or azimuthal polarization, depending on the waveplate's orientation. Formed structures were analysed with the use of scanning electron microscopy to define the optimal parameters for LIPSS formation. These findings provide a foundation for further studies of LIPSS formation using vector beams with varied polarization states. The modified GaAs surfaces exhibit distinct functional properties that could be used across a variety of applications.

Acknowledgments: Work was supported by Fundamental and Applied Research Project (Nr. lzp-2023/1-0199): "The Laser Photodetachment Spectroscopy on Negative Ions". We would like to express our sincere gratitude to K. Salmins and A. Sarakovskis for the help with acquiring the necessary equipment for experiments.

ERDF project No. 1.1.1.5/2/24/A/004

Machine learning solution for enabling cosmological analysis with the matter anisotropic three-point correlation function

Kristers Nagainis[1,2], Michele Moresco[1,2], Massimo Guidi[1,2], Antonio Farina[3,4,5], Alfonso Verapolumbo[3,4,5]

[1]*Institute of Astronomy, FST, University of Latvia, Latvia*
[2]*Dipartimento di Fisica e Astronomia "Augusto Righi"–Università di Bologna, Italy*
[3]*INAF - Osservatorio di Astrofisica e Scienza dello Spazio di Bologna, Italy*
[4]*Dipartimento di Fisica, Universit`a degli Studi di Genova, Italy*
[5]*INFN - Sezione di Genova, Italy*

e-mail: kristers.nagainis@lu.lv

The recent DESI results from the analysis of the DR2 [1] have significantly challenged the established LCDM model. Together with other Stage IV spectroscopic surveys, these missions will provide large volumes of data. They will probe the large-scale structures (LSS) of the Universe to a depth corresponding to when the Universe was only around 2 Gyr old. This allows to analyse the evolution of the Universe, including the components of it, such as dark matter and dark energy.

The most common way to analyse the LSS is to utilize the N-point correlation functions. The well-established two-point correlation statistics have proven to be a robust method for cosmological parameter constraints [2], exploiting the cosmic ruler: Baryonic Acoustic Oscillations (BAO). However, with the increase of the available data, two-point statistics are reaching their accuracy limits. Furthermore, they cannot distinguish non-gaussianity and suffer from parameter degeneracy. All of this can be alleviated by the inclusion of three-point statistics in the analysis.

The three-point correlation function (3PCF) has not been explored as well as the Fourier counterpart, the bispectrum. Nonetheless, it offers a significant advantage – it is not impacted by the survey footprint. One of the most recent theoretical advancements is the anisotropic 3PCF [3]. It is based on the Tripolar spherical decomposition, enabling to separate the anisotropic signal coming from the redshift space distortions and Alcock-Paczyński effect.

Although it is a very useful theoretical model, it takes a significant amount of computational resources to obtain it: approximately 30 CPU hours. Consequently, to constrain cosmological parameters with the Markov Chain Monte Carlo (MCMC) method, it could take years to finish the computation. To enable the cosmological analysis, I created an emulator, based on neural networks, that can speed up the computation by more than 10 million times, while maintaining competitive accuracy.

Furthermore, my MCMC analysis shows that including the anisotropic component yields more than 20% better constraints. This is only true when squeezed triangles are included in the analysis, thus $r_{min} = 20\ Mpc\ h^{-1}$. Otherwise, there is no significant improvement over the isotropic multipole constraints.

References

[1] Karim, M.A., Aguilar, J., Ahlen, S., Alam, S., Allen, L., Prieto, C.A., Alves, O., Anand, A., Andrade, U., Armengaud, E. and Aviles, A., 2025. DESI DR2 Results II: Measurements of Baryon Acoustic Oscillations and Cosmological Constraints. *arXiv preprint arXiv*:2503.14738

[2] Aghanim, N., Akrami, Y., Ashdown, M., Aumont, J., Baccigalupi, C., Ballardini, M., Banday, A.J., Barreiro, R.B., Bartolo, N., Basak, S. and Battye, R., 2020. Planck 2018 results-VI. Cosmological parameters. *Astronomy & Astrophysics*, 641, p.A6. [3] Atomic Spectra Database | NIST

[3] Sugiyama, N.S., Saito, S., Beutler, F. and Seo, H.J., 2021. Towards a self-consistent analysis of the anisotropic galaxy two-and three-point correlation functions on large scales: application to mock galaxy catalogues. *Monthly Notices of the Royal Astronomical Society*, 501(2), pp.2862-2896.

Tantalum pentoxide microring resonators

Kristians Draguns, Jānis Alnis

Institute of Atomic Physics and Spectroscopy, FST, University of Latvia

e-mail: kristians.draguns@lu.lv

We present our ongoing work on the design and development of high-quality-factor (Q) microresonators based on tantalum pentoxide (Ta_2O_5) [1], a CMOS-compatible material with high refractive index and wide bandgap, offering significant potential for nonlinear and quantum photonic applications. Our research focuses on the systematic optimization of microresonator geometries to tailor dispersion properties and enhance light confinement. The device design is carried out in-house, in collaboration with several international partners. Nanofabrication is performed at the University of Münster, ensuring precise control over waveguide and resonator dimensions. Measurement and characterization of the optical properties are conducted in collaboration with Riga Technical University, while dispersion characterization is performed in cooperation with the Max Planck Institute for the Science of Light. We report on recent advancements in resonator Q factors, modal analysis, and dispersion engineering strategies, laying the groundwork for efficient frequency comb generation and other nonlinear optical phenomena in the Ta_2O_5 platform.

Acknowledgments: The research was funded by the European Commission Recovery and Resilience Facility project Latvian Quantum Technologies Initiative (Grant No. 2.3.1.1.i.0/1/22/I/CFLA/001).

References

[1] Splitthoff, L., Wolff, M. A., Grottke, T., & Schuck, C. (2020). Tantalum pentoxide nanophotonic circuits for integrated quantum technology. Optics Express, 28(8), 11921. https://doi.org/10.1364/oe.388080.

ERDF project No. 1.1.1.5/2/24/A/004

The firms that break light.
A summary of statistics of the Photonics and Optics industry in Latvia in the last 5 years

Krišjānis Krakops

NSP FOTONIKA-LV, Latvia

e-mail: krisjanis.krakops@gmail.com

Photonics and Optics, two fields in physics that once held little interest about them beyond that of scientists and researchers, have both become key in modern advancements in technology. Their influence is pervasive, impacting nearly every facet of modern existence, from daily life and entertainment to critical sectors like medicine, defence, communications, and manufacturing. The mastery of light-based technologies is becoming inextricably linked to national progress and competitiveness. For small nations, often characterized by limited domestic market sizes, constrained natural resources, and the need for specialized economic niches, the photonics and optics industry present a unique and compelling strategic opportunity.

While large economies with substantial domestic markets and manufacturing scale often dominate high-volume segments of the global photonics and optics markets, the unique characteristics of this industry offer distinct strategic advantages and opportunities for smaller, more agile nations. The sectors high knowledge intensity, rapid pace of innovation, and diverse application landscape create avenues for specialisation where smaller countries can achieve global leadership in specific niche markets. Success for small economies in these fields typically hinges on focusing on high value-added products, services, and intellectual property, rather than attempting to compete on cost or volume in commoditised segments. This approach aligns well with the need for smaller economies to move up the global value chain and generate sustainable economic growth based on innovation rather than solely on resource exploitation or low-cost labour.

Central to harnessing these opportunities is the cultivation of a vibrant and supportive national innovation ecosystem. This requires a multi-faceted approach encompassing several key elements. **Strong foundational research capabilities**, typically housed within universities and public research institutes with specialized expertise in optics, photonics, materials science, and related engineering disciplines, are essential for generating new knowledge and seeding innovation. However, research alone is insufficient; **effective mechanisms for technology transfer are critical to bridge the gap between laboratory discoveries and commercially viable products**. This often involves dedicated tech transfer offices, incubators, science parks, and collaborative research programs designed to connect academic researchers with industry needs and entrepreneurial ventures.

Finally, targeted and consistent government support is often a crucial catalyst and enabler for developing a competitive photonics sector in smaller economies. This can take various forms, including direct funding for R&D programs, investments in shared research infrastructure, incentives for private sector R&D and innovation, support for skills development, facilitation of cluster initiatives, and the development of national strategies that prioritize photonics as a key sector.

Photonics and Optics in Latvia

What follows below is a summary of the key figures and trends in Latvia from the Photonics and Optics industries. Dated from 2014 till 2023 (data for 2024 is still largely unpublished) and encompassing a total of 54 firms, the figures show consistent growth in the 2 industries, in terms of people employed, turnover and overall profitability. Although some slowdown is observed in 2023, this can largely be attributed to macroeconomic factors outside the control of the industry and the overall trend remains positive.

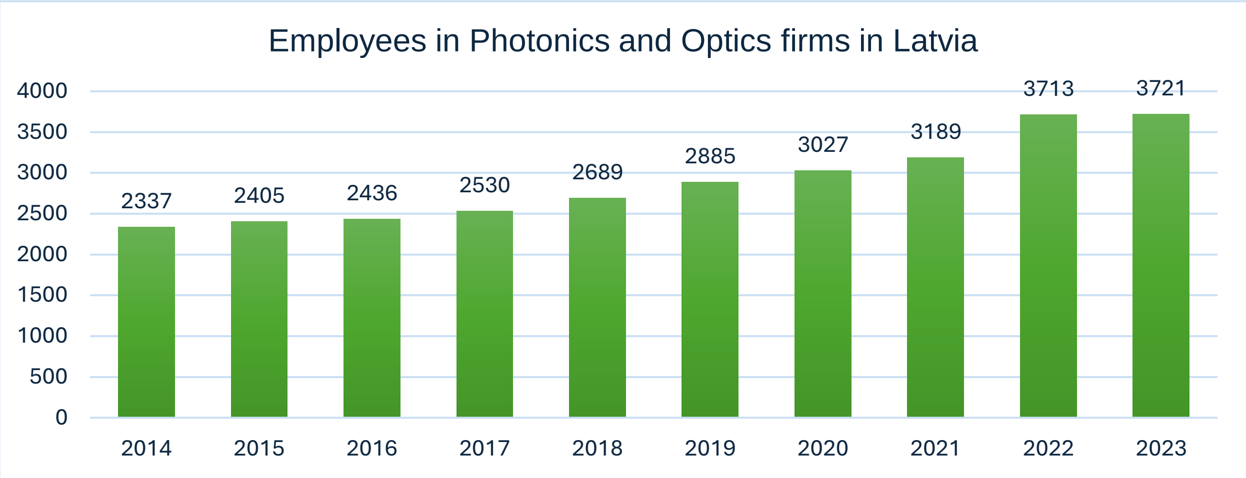

Figure 1. *Number of employees in the Photonics and Optics sector in Latvia from 54 firms sampled*

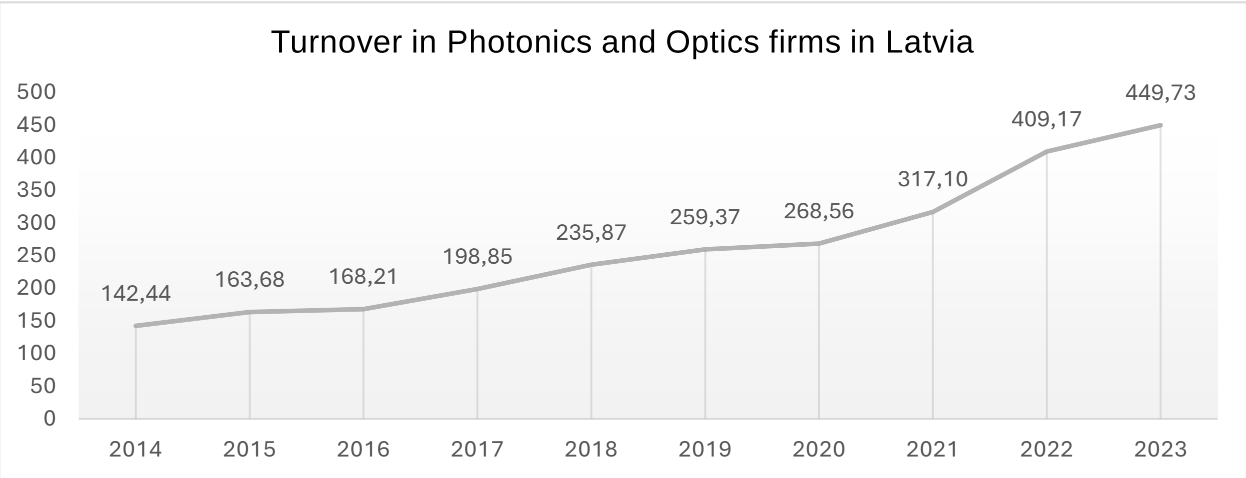

Figure 2. *Total Turnover in the Photonics and Optics sector in Latvia from 54 firms sampled*

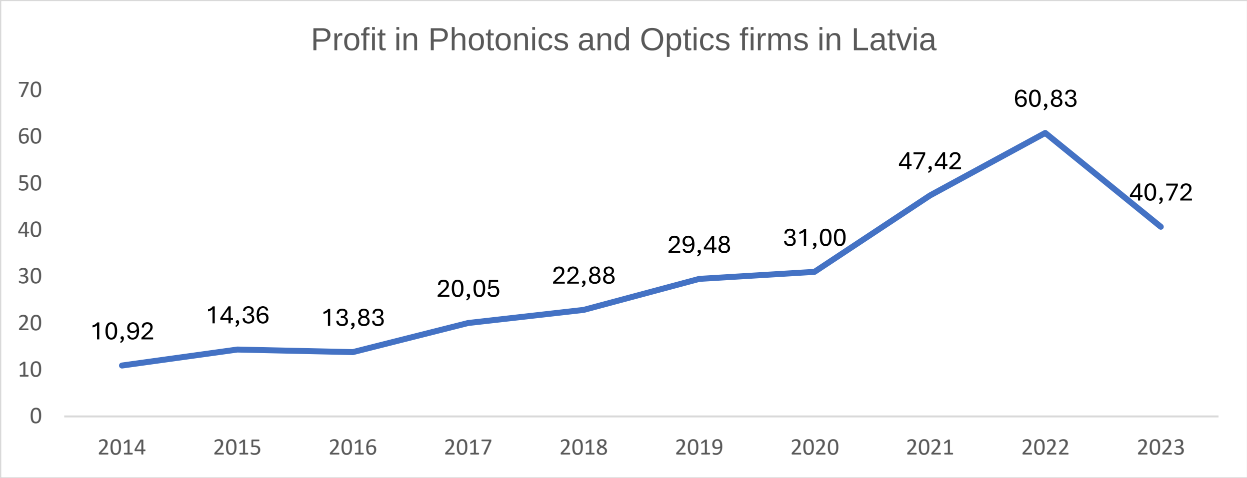

Figure 3. *Total Profit in the Photonics and Optics sector in Latvia from 54 firms sampled.*

References

[1] Latvijas Republikas Uzņēmumu reģistrs | https://info.ur.gov.lv/?#/data-search.

ERDF project No. 1.1.1.5/2/24/A/004

Spectroscopic studies of Gd I and Gd II using hybrid plasma source

Matīss Čakšs[1], Arnolds Ūbelis[2], Aleksandrs Koļesņiks[2], Juris Silamiķelis[2]

[1]Institute of Atomic Physics and Spectroscopy, FST, University of Latvia, Latvia,
[2]NSP FOTONIKA-LV, University of Latvia, Latvia

e-mail: matiss.cakss@lu.lv

This report shows results of spectroscopic studies of neutral gadolinium (Gd I) and ionized gadolinium (Gd II). A hybrid plasma source was used in this research: hollow cathode (HC) discharge combined with radiofrequency inductively coupled plasma (RF-ICP). Using this system plasma spectra from samples of Gd and Gd_2O_3 were produced and recorded. Analysis of recorded spectra indicate that both Gd I and Gd II are generated in the hybrid plasma source.

Measurements of metastable ion lifetimes

Uldis Bērziņš, Arturs Ciniņš

Institute of Atomic Physics and Spectroscopy, FST, University of Latvia, Latvia

e-mail: uldis.berzins@lu.lv

We will report on a series of works measuring the lifetimes of metastable levels for astrophysical interesting metastable ions. These experiments were carried out in close collaboration with the research group of Professor Henrik Hartman at Malmö University and the group led by Professor Henning Schmidt using the ion ring DESIREE [1] at Stockholm University.

Metastable levels are responsible for parity forbidden lines occurring in many low-density astrophysical plasmas, found in e.g. gaseous nebulae, planetary nebulae, protostars, stellar chromospheres. Line ratios from forbidden lines are the most reliable tools for diagnostics of temperatures and density of these regions. Measurements of metastable lifetimes is of direct importance for the use of forbidden lines.

We are using the laser probing technique what was derived by Mannervik [2] and his group at the CRYING storage ring and successfully applied to a number of ions of varying complexity [3]. For several complex ions the measured lifetimes can be combined with measured line ratios to derive experimental transition rates like it was done in our previous work [4].

We will report on preliminary results for Barium, Calcium, Nickel and Iron ions.

Acknowledgments: This research was supported by Fundamental and Applied Research Project (Nr. lzp-2023/1-0199): "The Laser Photodetachment Spectroscopy on Negative Ions", from Latvian Council of Science.

References

[1] H T Schmidt, et al. "First storage of ion beams in the Double Electrostatic Ion-Ring Experiment: DESIREE", Review of Scientific Instruments 84, 055115 (2013). https://doi.org/10.1063/1.4807702

[2] Mannervik, S, Studies of Metastable Levels in Singly Charged Ions by Laser Techniques in an Ion Storage Ring, Physica Scripta, Volume 100, pp. 81-87 (2002)

[3] Hartman, H, Johansson, S, Lundberg, H, Lundin, P, Mannervik, S, Schef, P, Experimental Oscillator Strengths for Forbidden Lines in Complex Spectra, Physica Scripta, Volume T119, pp. 40-44 (2005)

[4] U. Berzins, A. Ubelis, and A. Bziskjans, 'Branching Fraction Measurements of Arsenic 4p25s-4p3 Transitions', JQSRT 271, 107943 (2021).

ERDF project No. 1.1.1.5/2/24/A/004

Coherent control in size selected semiconductor quantum dot thin films

Victor Kärcher[1], Tobias Reiker[1], Pedro F.G.M. da Costa[2], Andrea S.S. de Camargo[3,4], Helmut Zacharias[1]

[1]Center for Soft Nanoscience, University of Münster, Germany
[2]São Carlos Institute of Physics, University of São Paulo, Brazil
[3]Federal Institute for Materials Research and Testing (BAM), Berlin
[4]Friedrich-Schiller University Jena (FSU), Germany

e-mail: v_kaer01@uni-muenster.de

Quantum interference [1] is a cornerstone phenomenon in quantum mechanics, arising when the probability amplitudes associated with different quantum pathways combine, leading to patterns of constructive or destructive interference. Coherent control [2] leverages this phenomenon by using external optical or electromagnetic pulses to steer the outcome of quantum interference. Through careful adjustment of the phase, amplitude, and frequency of these external pulses, it is possible to selectively enhance or suppress specific quantum transitions. This selective manipulation enables researchers to direct quantum pathways toward desired outcomes, making coherent control a powerful tool for exploring and utilizing quantum systems.

In this study [3], we present a novel approach to coherent control by exploiting resonant, internally generated fields within CdTe quantum dot (QD) thin films at the L-point in the Brillouin zone (see Fig. 1. CdTe is chosen for its favourable electronic properties, including a bulk band gap of 3.6 eV at the L point, where transitions are strongly influenced by Coulomb interactions. Third harmonic generation (THG) is employed, with a third harmonic wavelength of λ 3 = 343 nm (hv = 3.61 eV) driven by a fundamental wavelength of λ 1 = 1030 nm. This resonant condition allows precise control of three-photon pathways connecting the valence and conduction bands. The experimental setup leverages CdTe QD films of varying thicknesses to finely tune the phase relationship between the fundamental external field and the internally generated third harmonic field. This tuning enables the suppression or significant enhancement of resonant third harmonic signals (see Fig. 2), while the non-resonant harmonic contributions remain largely unaffected. Such control is achieved by modifying the quantum interference patterns between different photon pathways. By using high peak intensities, we induce an increased population of conduction band electrons, which alters the refractive index of CdTe. This change enhances the phase mismatch between the fundamental and third harmonic fields, reducing the coherence length from the micrometer to the nanometer scale. This technique introduces an additional layer of control over quantum interference through phase manipulation at ultrafast timescales. The implications are far-reaching, offering potential applications in ultrafast switching, quantum cryptography, and the development of next generation nanophotonic devices. By bridging the gap between fundamental quantum mechanics and practical device applications, this work underscores the potential of quantum interference as a foundational tool in the rapidly evolving field of quantum technologies.

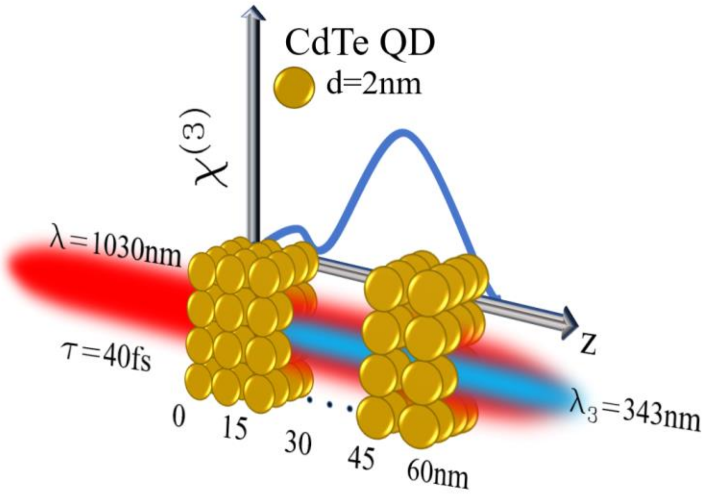

Figure 1: *Schematic representation of the experiment. In order to coherently control the resonant nonlinear susceptibility different CdTe QD film thicknesses are used*

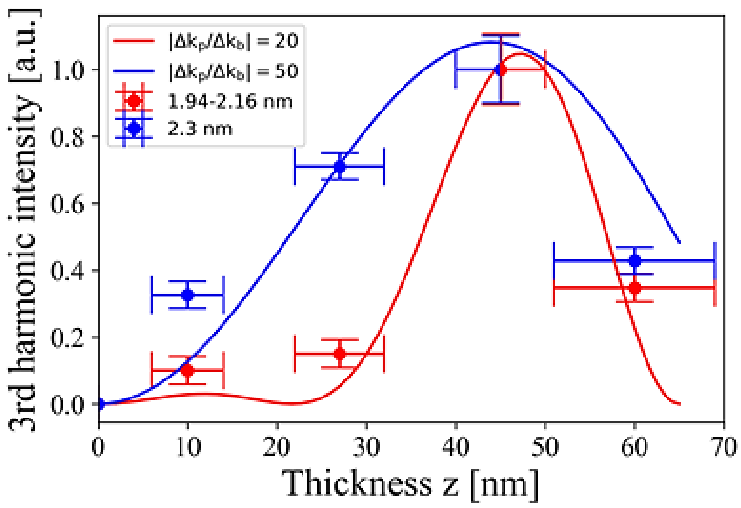

Figure 2*: Coherent control of the resonant third harmonic intensity at* $h\omega_3$ *= 343 nm is demonstrated*

References

[1] E. A. Manykin and A. M. Afanas'ev, "On one possibility of making a medium transparent by multiquantum resonance," J. Theor. Phys., 52, pp. 1246–1250 (1967) , Sov. Phys. JETP, 25, no. 5, p. 828 (1967)

[2] D. Dong and I.R. Petersen, "Quantum control theory and applications: a survey," IET Control Theory Appl., 4, pp. 2651–2671 (2010)

[3] V. Kärcher, T. Reiker, P. da Costa, A. de Camargo, and H. Zacharias, "Quantum control in size selected semiconductor quantum dot thin films," Nanophotonics, https://doi.org/10.1515/nanoph-2024-0529 (2025).

ERDF project No. 1.1.1.5/2/24/A/004

The effect of EM levitation, pressure and temperature combination on synthesizing the Magnesium – high Titanium alloys

Viesturs Silamiķelis, Aigars Apsītis, Jānis Blahins, Austris Pumpurs, Jānis Sniķeris, Ashish Kumar Singh

Institute of Atomic Physics and Spectroscopy, FST, University of Latvia, Latvia

e-mail: viesturs.silamikelis@gmail.com

Magnesium metal is widely used – the World`s third most applied metal - both in the form of ingots or in mechanical processing. Currently, it is the lightest technological metal resistant to corrosion under normal conditions with a 5% increase in use yearly. In alloys with aluminium, it can be easily produced in very wide proportions. With zinc it can be achieved as an additive to zinc alloys, since pure magnesium alloys are characteristic by low thermal stability. Pure magnesium burns in air and actively reacts with water, nitrogen, carbon dioxide, which at temperatures above 500ºC is the most significant problem of magnesium and its alloys, in spite of magnesium alloys are even more strong than popular aluminium alloys. In turn, in alloys with titanium, only 0.2% titanium allows to observe a noticeable improvement in mechanical properties. There are known experiments with powder technologies with up to 99% titanium, where an increase in hardness is observed, however, it is strongly harmed by the brittleness inherent in ceramics - however, thermal safety is significantly increased.

Under normal conditions (at 1 bar pressure), it is impossible to achieve the formation of an alloy, because as soon as the addition of titanium exceeds 0.2%, the melting point of the alloy increases above 1090ºC and all magnesium boils away - its boiling point is 1090ºC. This has slowed down the research of Mg-Ti alloys with higher titanium concentration, shifting the emphasis to powder metallurgy and other technologies. The melting point of pure titanium is 1670ºC. Under normal pressure conditions, there are two modifications - α and β with a transition at 882ºC. Magnesium is a chemically very active metal and, when molten, reacts rapidly with O_2, N_2, CO_2, water and also with crucible materials, depriving them of oxygen, phosphorus, nitrogen in ceramic crucible materials or even reacting with graphite. This makes melting magnesium at temperatures above 1000ºC problematic. But there exists a little-known fact that gives strong hope for synthesizing a new type of magnesium-titanium alloy without of any ratio restrictions.

1. We do not use a crucible at all in electromagnetic levitation (EML) - the molten metal is held by the electromagnetic field. We have already implemented magnesium melting in levitation in an argon protective atmosphere in LU-ASI, Šķūņu street 4 laboratory in previous works. We have also implemented the levitation of titanium melts.
2. High-pressure melting solves the problem of magnesium boiling. The partial pressure of magnesium vapor at the melting point of titanium 1670ºC is 18 bar.
3. It is possible to build a box for pressure up to 50 bar in which to implement EML.

Why to try? Such an alloy would be the lightest of any metal (almost 2x lighter than aluminium), and also a metal that is stable in the atmosphere thanks to titanium. It has to be relatively cheap because magnesium is widespread in nature. It has to be significantly more durable than aluminium - with potential applications in aviation and the space industry, as well as in medicine -

so that the benefit to the national economy would be high. Latvia is very rich in dolomite, of which almost a third is magnesium carbonate. There are known several developed technologies for extracting magnesium from dolomite. True, purification is bound with energy-intensive manufacturing and potentially harmful by-products - calcium, chlorine, CO_2, etc., yet which can be recycled and even converted into useful by-products if due resources are invested in science. Latvia has the opportunity to become great again and give the world something new and highly valuable.

ERDF project No. 1.1.1.5/2/24/A/004

Investigating the Impact of Hollow Cathode Lamp Geometry on Neodymium Emission Spectra

Pratyush Ranjan Sen Sarma, María Teresa Belmonte, Santiago Mar

Department of Theoretical, Atomic Physics and Optics, University of Valladolid, Spain

e-mail: pratyush.ranjan.sen.sarma@uva.es

Introduction

Spectroscopic investigations of rare earth elements, such as neodymium, are essential to a broad range of fields, including astrophysics [1], quantum information science [2], and advanced lighting technologies [3]. Laboratory-generated plasmas, when operated under controlled conditions, serve as reliable sources for the precise determination of atomic parameters, including transition probabilities. In our laboratory, we utilise a hollow cathode lamp (HCL) - a well-established plasma source in high-resolution spectroscopy [4] - to experimentally determine transition probabilities for doubly ionized neodymium (Nd III). Such measurements are particularly important for refining astrophysical data, where Nd III lines play a critical role [5].

Since plasma conditions affect the signal-to-noise ratio (SNR), the accuracy of these measurements is strongly dependent on the discharge parameters, which are, in turn, influenced by the geometric configuration of the lamp - particularly the anode design.

Experimental Setup

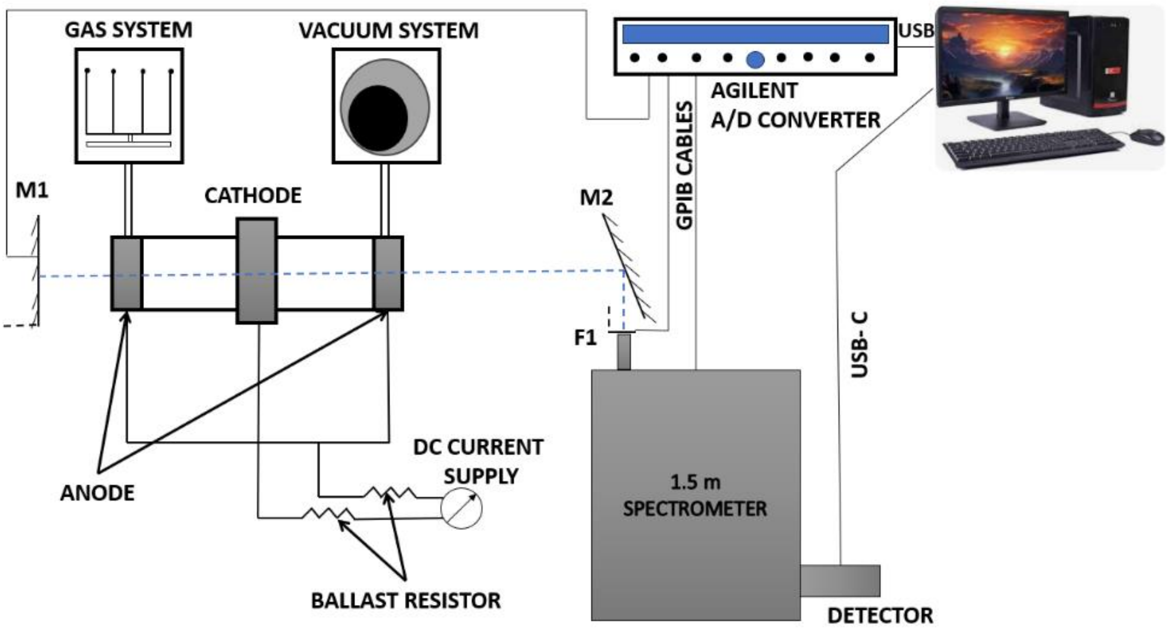

Figure 1. *Schematic diagram of the experimental setup. Mirror M1 positioned at the back of the lamp is used to reconstruct the self-absorbed spectral lines [4]. Flap F1 is positioned to block light from reaching the spectrometer during background signal measurements, otherwise, it is retracted to the position indicated by the dotted lines. The motorised movements of M1, F1, and the spectrometer grating are synchronised and controlled by an Agilent analogue-to-digital (A/D) converter connected to the computer via GPIB*

The Atomic Spectroscopy Laboratory at the University of Valladolid (Spain) has a long history in plasma spectroscopy [4, 6-8], initially focusing on noble gases [4] and more recently expanding to rare earth elements such as neodymium. This expansion is driven by the element's significance in stellar abundance studies and the lack of accurate atomic data for neodymium in the NIST Atomic Spectra Database [9].

A schematic of the experimental setup is shown in Fig. 1. At the heart of the system is a hollow cathode discharge lamp, featuring a cylindrical neodymium cathode (10 mm outer diameter, 20 mm length). The discharge is sustained in an argon buffer gas environment, introduced at pressures between 30–50 Pa, following evacuation to a base pressure of approximately 10-2 Pa. A DC power supply (0–1000 V, up to 1 A), coupled with ballast resistors, maintains a stable discharge. The emitted light is collected and directed into a 1.5 m Jobin-Yvon HR1500 Czerny–Turner spectrometer equipped with a 2400 lines/mm diffraction grating. Spectral detection is performed using a PCO.edge 4.2 CMOS camera with a pixel size of 6.5 × 6.5 μm². Plasma emission is imaged onto the spectrometer entrance slit using an alignment mirror (labelled M2). Inside the spectrometer, optics guide the spectral emission to the CMOS detector, where the spectra are recorded [10] for subsequent analysis.

The mechanical components of the experiment are controlled via a computer interface using an Agilent A/D converter and GPIB cables. Detailed descriptions of the experimental setup can be found in references [11] and [12].

This study investigates the effects of anode geometry on the plasma characteristics and emission behaviour of Nd III. In this poster we will present modifications to the lamp design, an updated voltage–current discharge profile, and comparative analyses of emission spectra and plasma glow images to visualise the impact of these geometric changes.

Acknowledgments: This work was conducted under the Spanish government through project PID2021-127786NA-100 funded by MICIU/AEI /10.13039/501100011033 and by FEDER, UE. P. R. Sen Sarma thanks the University of Valladolid for his PhD grant. M. T. Belmonte acknowledges the Beatriz Galindo Fellowship from the Ministerio de Ciencia, Innovación y Universidades of the Spanish Government.

References

[1] Banerjee, S., Cassisi, S., Colgan, J., Fontes, C.J., Frey, H.M., Kelley, K., Lippuner, J. and Miller, R.H. (2022). Opacity of the highly ionized lanthanides and the effect on the early kilonova. The Astrophysical Journal, 934(2), p.117

[2] Goldner, P., Ferrier, A. and Guillot-Noël, O. (2015). Rare earth-doped crystals for quantum information processing. In: J.-C.G. Bünzli and V.K. Pecharsky, eds. Handbook on the Physics and Chemistry of Rare Earths. Vol. 46. Amsterdam: Elsevier, pp.1–78

[3] Song, X., Chang, M.-H. and Pecht, M. (2013). Rare-earth elements in lighting and optical applications and their recycling. JOM, 65, pp.1276–1282

[4] Belmonte, M.T., Aparicio, J.A, and Mar, S. (2014). Improved and expanded measurements of transition probabilities in UV Ar II spectral lines. Monthly Notices of the Royal Astronomical Society, 445(4), pp.3345–3351

[5] Hasselquist, S., Shetrone, M., Cunha, K., Smith, V.V., Holtzman, J., Lawler, J.E., Prieto, C.A., Beers, T.C., Chojnowski, D., Fernández-Trincado, J.G. and García-Hernández, D.A. (2016). Identification of Neodymium in the Apogee H-Band Spectra. The Astrophysical Journal, 833(1), p.81

[6] Belmonte Sainz Ezquerra, M.T. (2016). Experimental transition probabilities and stark parameters of singly ionized noble gases. Doctoral Thesis, University of Valladolid

[7] Mar, S., Aparicio, J.A., Calisti, A., Ćirišan, M., de La Rosa, M.I., del Val, J.A., Djurović, S., Fuentes, L.M., Gigosos, M.A., González, M.Á. and Gonzalo, A.B. (2011). Research areas of the Plasma Spectroscopy Group at the University of Valladolid. Óptica pura y aplicada, 44(3), pp.433-445

[8] Peláez, R.J., Mar, S., Aparicio, J.A. and Belmonte, M.T. (2012). Integration of an intensified charge-coupled device (ICCD) camera for accurate spectroscopic measurements. Applied Spectroscopy, 66(8), pp.970-978

[9] Kramida, A., Ralchenko, Y., Reader, J. and NIST ASD Team (2024). NIST Atomic Spectra Database (version 5.12) [online]. Gaithersburg, MD: National Institute of Standards and Technology. Available at: https://physics.nist.gov/asd [Accessed 8 Apr. 2025]. doi:10.18434/T4W30F

[10] Sen Sarma, P.R., Belmonte, M. T. and Mar, S. (2024) "Analysis of Slit Curvature Using Image Processing". Zenodo. doi: 10.5281/zenodo.14002840

[11] Sen Sarma, P.R., Belmonte, M.T. and Mar, S. (2024). Characterisation of a hollow-cathode lamp to measure accurate branching fractions of rare-earth elements. The European Physical Journal D, 78(6), p.76

[12] Sen Sarma, P.R., Belmonte, M.T., Llorente, S. and Mar, S., Integration of a CMOS camera for accurate high resolving power spectroscopic measurements. SSRN. Available at: https://ssrn.com/abstract=5018907 [Accessed 8 Apr. 2025].

Līdzfinansē Eiropas Savienība
2027 Nacionālais attīstības plāns
ERDF project No. 1.1.1.5/2/24/A/004
LATVIJAS UNIVERSITĀTE
FOTONIKA-LV
NATIONAL SCIENCE PLATFORM AT THE UNIVERSITY OF LATVIA

Interdisciplinary Laser Spectroscopy - The interplay between basic and applied sciences and resulting industrial impact

Sune Svanberg

Department of Physics and Lund Laser Centre, Lund University, Sweden

e-mail: sune.svanberg@fysik.lth.se

Laser spectroscopy, enabled by continuing strong advances in quantum electronics and the development of new spectroscopic concepts, is having a profound impact on wide sectors. These include fundamental sciences, applied research and industrial spin-off (see, e.g., [1], Chapters 8-10). Sometimes, and in particular historically, these different aspects have been considered contradictory, but a unified view, that there is a continuous and healthy transition between these different aspects is emerging. Frequently, there appear very important and totally unexpected applications of seemingly exotic basic research [2]. The speaker will illustrate the interplay between basic, applied, and resulting industrial activities based on own experience [3], mostly from the platform of the Lund Laser Centre.

References

[1] S. Svanberg, Atomic and Molecular Spectroscopy – Basic Aspects and Practical Applications, 5th edition, Springer-Nature (2022) https://link.springer.com/book/10.1007/978-3-031-04776-3

[2] J. Bergström, G. Holm, J. Håstad, G. Ingelman, U. Lindahl, T. Norin, The Unexpected Usefulness, Royal Swedish Academy of Sciences (2012) (Den Oväntade Nyttan, in Swedish) https://www.kva.se/app/uploads/2022/06/ovantadenyttan170831.pdf

[3] S. Svanberg, Physics – Curiosity and Usefulness, in the Swedish Physical Society Yearbook KOSMOS 2024 (Fysiken – Nyttan och Nyfikenheten, in Swedish) https://www.fysikersamfundet.se/wp-content/uploads/Kosmos-sartryck-2024-1-Svanberg72.pdf.

ERDF project No. 1.1.1.5/2/24/A/004

Laser Spectroscopy of Negative Ions

Uldis Bērziņš

i Institute of Atomic Physics and Spectroscopy, FST, University of Latvia, Latvia

e-mail: uldis.berzins@lu.lv

I will report on the results and conclusions of the first year of work in the Latvian Science Council project (No. lzp-2023/1-0199): "Negative ion laser photodetachment spectroscopy". The main goal is to obtain more information and better understand the structure and dynamics of atomic systems in them. We do this in collaboration with scientists from CERN [1] in Switzerland and three Swedish universities from Gothenburg [2], Malmö [3] and Stockholm [4]. The basic idea of the project is to conduct high-class experiments during short scientific visits to the large laboratories CERN and DESIREE. Preparatory work and processing of the results are carried out at the Institute of Atomic Physics and Spectroscopy [5].

Top-level research and innovation are most intensively developed in large scientific laboratories. They have access to expensive equipment and complex infrastructure that Latvia cannot afford to purchase and maintain. Conducting research on such modern equipment allows both experienced researchers and young scientists to grow and achieve world-class results.

Work in large centres is very different from the usual routine. In them, we have to pass a competition for access to the facility with our experimental idea. In case of success, such access is given. One or two weeks to carry out the planned experiments. During this time, the operation of the experimental facility is provided by the host laboratory, both financially and with personnel. We only need to find a budget for travel and accommodation. But it is very important to prepare a completely clear work plan, because when the allotted time runs out, the second opportunity may be only after a year, or not at all.

The report will present the results of recently conducted experiments on the lifetime of positive ions and the energies of electron detachment from negative ions. 3 conclusions to be drawn at this time are:

- it is very important that all project participants are able to participate in experimental missions.
- funding for business trips is too little planned
- the problem is the complicated and slow procurement procedure at the University of Latvia.

Acknowledgments: This research was supported by Fundamental and Applied Research Project (Nr. lzp-2023/1-0199): "The Laser Photodetachment Spectroscopy on Negative Ions", from Latvian Council of Science.

References

[1] https://home.cern/science/experiments/isolde
[2] https://www.gu.se/om-universitetet/hitta-person/daghanstorp
[3] https://mau.se/en/persons/henrik.hartman/
[4] https://www.desiree-infrastructure.com/desiree
[5] https://www.lu.lv/par-mums/struktura/instituti/lu-atomfizikas-un-spektroskopijas-instituts/.

ERDF project No. 1.1.1.5/2/24/A/004

Advances in Application of Hybrid system: Hollow Cathode and Low Temperature Inductively Coupled Plasma for Spectroscopic Investigation of Basic Properties of Atoms and Ions of Hardly Volatile Elements

Arnolds Ūbelis

NSP FOTONIKA-LV, University of Latvia, Latvia

e-mail: arnolds@latnet.lv

The presentation will highlight the game changing potential of hybrid plasma technology (hollow cathode discharge & inductively coupled radiofrequency plasma: RF-ICP & HC) in UV, VUV spectroscopy research to address the pressing need for novel insights and expertise in pertinent fields:

- valuable for astrophysics in treatment of spectroscopic data captured by emerging “after Hubl” fleet of space telescopes [1], [2], [3], [4],
- will provide response to the urgent need, faced by modern atomic physics and its theoretical frameworks, for new and/or improved empirical data on UV, VUV spectroscopy, and basic properties of scarcely investigated atoms and ions [5],
- will make progress in the development of calibration tools, frequency standards [6], and intense UV/VUV spectral line sources for UV-C light, crucial for the Photonics.

Application of hybrid plasma technology open a lot of possibility, for the first time, to study excited by RF- ICP plasma emission spectra of atoms of hardly volatile elements, as well as ions of many elements. The research team see possibility to study emission spectroscopy of Se II likewise that was done for Se I [7].

References

[1] Anil K. Pradhan, Sultana N. Nahar. Monography. Atomic Astrophysics and Spectroscopy. Cambridge University Press; 2011. 376 pages

[2] Uldis Bērziņš. Combination of 3 Different Measurements: Branching Fractions, Radiative Lifetimes, and Absorption Oscillator Strengths - a Good Opportunity for the Analysis of the Presence of Elements in Astrophysical Objects. Conf. paper. Measurement 2021 Conference. 17-19 May 2021, Slovakia

[3] After Hubble: This Canadian telescope could fill coming 'ultraviolet gap'. News, by Elizabeth Howell, published December 11, 2023: https://www.space.com/hubble-space-telescope-ultraviolet-gap-canada-castor-telescope

[4] PLAnetary Transits and Oscillations of stars (PLATO) is a space telescope under development by the ESA for launch in 2026: https://www.esa.int/Science_Exploration/Space_Science/Plato_factsheet

[5] Advances in Atomic Physics: An Overview, by Nobel Prise Laureate Claude Cohen-Tannoudji, and David Guery-Odelin. (2011) World Scientific Illustrated, Kindle Edition, 794 pages

[6] B..L.Schmittberger, D. Scherer. A Review off Contemporary Atomic Frequency Standards. arXiv:2004.09987v1 [physics. atom-ph] 21 Apr 2020, 18 pages: https://arxiv.org/pdf/2004.09987

[7] Ubelis, A. P., & Berzinsh, U. V. (1986). Transition probability measurements of Se I spectral lines by emission method. Physica Scripta, 34(6B), 805-806.

ERDF project No. 1.1.1.5/2/24/A/004

Laboratory Atomic Spectroscopy for stellar and kilonova astrophysics

Henrik Hartman

Faculty of Technology, Malmö University, Sweden

e-mail: henrik.hartman@mau.se

Astronomical spectra provide the vast majority of information that we know of the objects in the universe. These diagnostics are possible from detailed knowledge of the structure of the atomic species involved. In addition, the line strengths must be accurately known to use astronomical spectra for quantitative analyses, such as the determination of stellar and nebular temperatures, ion and electron densities, and ultimately chemical abundance. Spectral regions provide insight to different processes, but also different objects, since the emission and absorption have various spectral imprints. In recent years, the near-infrared wavelength region, 1–5 μm, is becoming more important thanks to its smaller interstellar extinction and several new spectrographs are coming online matching these needs. The planned European Extremely Large Telescope (E-ELT) will observe predominantly in the infrared domain. The lack of atomic data for the near-infrared region will appear in this case. Stellar surveys in the optical region rely on accurate transitional data to fully exploit the expensive observations.

Our research program on Laboratory Atomic Astrophysics focuses on the needs atomic data, both line identification and measurements of intrinsic line strengths, the oscillator strengths. This includes both the infrared and optical transitions.

We will review the branching fraction and lifetime technique to measure line strengths, using the high-resolution Fourier spectrometer at Edlen Laboratory at Malmö university, in combination with radiative lifetimes. The measurements are combined with calculations using the GRASP and ATSP2k codes, providing a high-accuracy data set for astrophysical analysis.

In the present contribution, I will discuss infrared transitions from an atomic structure point of view and as a base for the astronomical analysis as well as for laboratory and theoretical priorities. Examples are given from recent studies on Sc I, Mg I, Al I, Si I and La I for the stellar studies. In addition, I will present our project on high-precision lifetime measurements of metastable states, performed at the DESIREE storage ring.

A more recent application is the detection of a kilonova, the afterglow from a binary neutron star merger, in 2017. To decipher these spectra, atomic data for the heavy neutron-capture elements is needed. I will present our work in this area.

ERDF project No. 1.1.1.5/2/24/A/004

The application of laser-induced breakdown spectroscopy for analysis in ores from deep boreholes in Latvia

Vyacheslav Kim[1], Rashid Ganeev[2], Arnolds Ūbelis[2], Dainis Ozols[3]

[1]Institute of Fundamental and Applied Research under the National Research University
[2]NSP FOTONIKA-LV, University of Latvia, Latvia
[3]Professional Association "Ziemeļvidzemes ģeoparks", Latvia

e-mail: arnolds@latnet.lv

The aim of reported research agenda, to clarify the potential to enrich knowledge base on the presence of various elements and precious metals [1] up to trace level in geological structures of Latvia via renewed studies of deep (up to 1,2 km) boreholes using the advanced and very sensitive LIBS methodology and the experience obtained by the applicant and the team of colleagues in the first pilot studies [2], [3], [4] LIBS is a simple, straightforward, versatile, and highly sensitive form of atomic emission spectroscopy that focuses a rapidly pulsed laser beam onto a sample to form a plasma containing its constituent elements and then uses spectral analysis of the emitted light to detect the elements present. To date, LIBS has been rarely used in geological material studies, despite its advantage of directly and rapidly identifying trace elements in samples. It requires no intermediate steps or time-consuming preconcentration procedures. The application of LIBS methodology is particularly valuable as a first attempt and an effective tool for microscale geochemical mapping in deep boreholes within the crystalline geological structures of Latvia. This will mark the first national-wide application of LIBS technologies for deep boreholes with the potential for game changing outcomes that could shed light on the finer details of Latvia's still underexplored geological structures.

The crystalline basement rocks of Latvia have been considered unpromising for practical use [5] due to significant depth – 300-1900 m (iron ores 400-1000 m). However, nowadays valuable metals such as gold, silver, platinum, and even copper and nickel are mined in shafts reaching depth of 2-4 km. Manganese (to 18% in Staicele deposit) and cobalt (to 0,7% in Gārsene deposit) previously found in the iron ores in 1980-1990-ties today is in the list of critical materials of the European Union, see [6]. If the quantity of metals reaches mineable limits and the ore quality is good, the above-mentioned depth is not and obstacle for their practical use.

Application of LIBS methodology likely will become game changing contribution in creation of a complete picture about the of diversity of chemical elements in the crystalline basement ores in Latvia. It is valuable and exclusive addition to methods used by researchers of the above-mentioned project.

References

[1] List of Critical Raw Materials is named for 2023 in the European Union report: European Commission, Study of Critical Raw Materials for the EU 2023 - Final Report

[2] Ganeev, R. A., Kim, V. V., Vorobyov, D., Gross, U., Ubelis, A., Ozols, D., & Sarakovskis, A. (2024). The First Application of Laser-Induced Breakdown Spectroscopy: A Fast-Analytical Technique in Targeted Search for Elements in Geological Samples from Deep Boreholes in Latvia. Latvian Journal of Physics and Technical Sciences, 61(2), 23-32

[3] Rashid A. Ganeev, Vyacheslav V. Kim, Jelena Butikova, Aigars Atvars, Jurgis Grube, Anatolijs Sarakovskis, and Arnolds Ubelis, (2023) "High-order harmonics generation in Cd and Pd laser-induced plasmas," Opt. Express 31, 26626-26642 (2023)

[4] V.V. Kim, J. Grube, J. Butikova, *et al*. Influence of chromium plasma characteristics on high-order harmonics generation, Appl. Phys. B 128, 217 (2022)

[5] Brangulis, J.A., Kuršs, V., Misāns, J., Stinkulis, Ģ. 1998. Latvijas ģeoloģija (Geology of Latvia). State Geological survey of Latvia, Riga Vetrennikov, V. 1991. Zhelyezisto-kremn'istye formacii dokembriya Latvii i ikh prognoznaya ocenka (Ferruginous and siliceous formations in the Precambrian of Latvia and their orecastin evaluation). Riga, Zinatne (in Russian)

[6] Vetrennikov, V. 1991. Zhelyezisto-kremn'istye formacii dokembriya Latvii i ikh prognoznaya ocenka (Ferruginous and siliceous formations in the Precambrian of Latvia and their forecasting evaluation). Riga, Zinatne (in Russian).

ERDF project No. 1.1.1.5/2/24/A/004

title

name

institute

e-mail:

…

…

…

Acknowledgments
This research was funded by ….

References

[2] ….

ERDF project No. 1.1.1.5/2/24/A/004

Four-level Generation in Laser-Induced Plasma Lasers

Lev Nagli, Kirill Kulikov, Dima Cheskis

Ariel University, Ariel 4000, Israel

e-mail: levna@ariel.ac.il

Laser-induced plasma lasers (LIPL) have been extensively studied in the Laser Spectroscopy Lab of Ariel University. We demonstrate that stimulated emission and lasing occur under appropriate resonant and **linearly polarized** optical pumping of a pre-formed laser-induced plasma (LIP) plume. It manifests as the emission of intense, collimated, and **polarized** beams. A relatively small external magnetic field governs the polarization of the LIPLs generation. We call this effect Laser-Induced Plasma Lasers (LIPLs). We investigated LIPLs generated according to the 3-level scheme (the 13^{th} group elements) [1-4] and according to the quasi-three-level scheme, which we nominate as a Direct Generation (**DG**) scheme (mostly elements from the 14^{th} group) [5,6].

The present talk explores the four-level generation in LIPLs, where lasing occurs between intermediate energy levels. The upper generation level Eu is inversely populated from the pumped level E_p through fast electron impacts (**IP**) and IR radiative transitions. The two cases are distinguished based on the energy difference $\Delta E=E_p-E_u$: (i) a large $\Delta E\approx 1$ eV, and (ii) a small $\Delta E\approx 0.1$ eV. In this case of $\Delta E\approx 1$ eV, there are numerous intermediate energy levels between E_p and E_u. Achieving population inversion at the E_u level requires collisional processes to transfer population effectively through these intermediate levels. The mechanism of these collisional processes and the potential role of direct infrared (*IR*) generation transitions from E_p to E_u are discussed in the presentation. When the energy gap is small, there may be few or no intermediate levels between E_p and E_u . This leads to an effective coupling of E_p and E_u to one level simplifying the population inversion process. In this scenario, the generation process is discussed within the framework of the direct generation (DG) scheme as outlined in reference [6].

The experimental setup is presented in [7]. Here we only emphasize that the pumping OPO generation is vertically polarized, and the polarization of the LIPL was measured relative to the OPO polarization vector $\boldsymbol{E_p}$. The degree of generation polarization (DOP) was used as a measure of polarization, defined as:

$$\boldsymbol{DOP} = \frac{(I_{II} - I_{\perp})}{(I_{II} + I_{\perp})} \quad , (1)$$

where $\boldsymbol{I_{\parallel}}$ and $\boldsymbol{I_{\perp}}$ represent the generation-line intensities with the electric vector $\boldsymbol{E_g}$ parallel and perpendicular to $\boldsymbol{E_p}$, respectively.

Fig. 1 a presents *Ti* LIPL under pumping at 230.27nm as a typical four-level generation with large ΔE (≈0.7eV). Under this pumping, the DG is observed at 1688 nm (E_p=E_u=5.404 eV), alongside four-level generation lines at 548.14 nm and 622.04 nm (with E_u =4.669 eV for both). The generation lines at 1688 nm and 547.77 nm are strongly polarized with a positive DOP, while the 622.04 nm line is polarized with a negative DOP. The external magnetic field of 280 mT parallel to the direction of the generation strongly diminishes generation polarization. Fig. 1b presents these generations' transitions scheme.

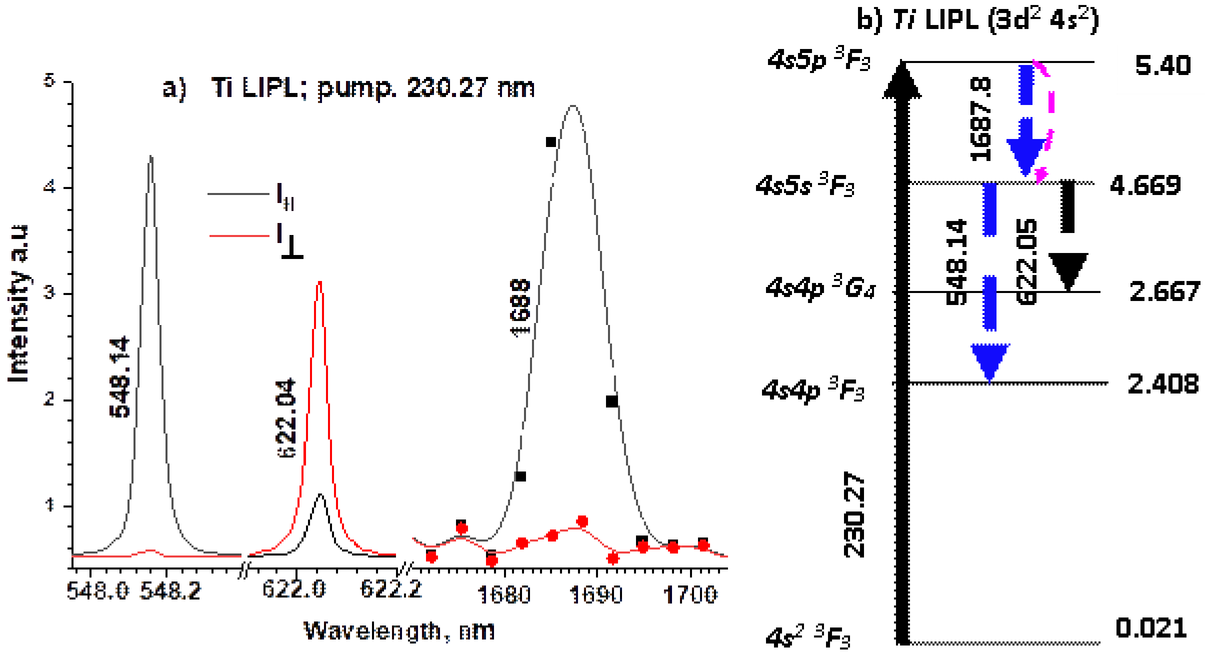

Figure 1. *a) Four-level polarized generation spectra for Ti LIPL under pumping at 230.27 nm; b) Energy scheme for these generations*

The black upward-pointing arrow represents the pumping transition. Violet curved arrows indicate collisional transitions. Dashed blue and black arrows pointing downward represent lasing with positive and negative DOP, respectively. The numbers along the arrows correspond to the pumping and generation wavelengths, and the numbers to the right of the levels represent energy in eV

Two pathways for the creation of the inversion population on the E_u level due to collisionally assistant transitions are discussed in the example of the *Ti* LIPL pumped at 229.99 nm: The first is the cascade EI energy loss involving **all** intermediate levels between $\boldsymbol{E_p}$ and $\boldsymbol{E_u}$ levels. The second one is the one-step collisionally assistant jump from the $\boldsymbol{E_p}$ level to the $\boldsymbol{E_u}$ level.

Fig.2 presents the energy scheme of the *Ti* LIPL pumped at 299.99 nm, which was used for estimating models of the E_u inverse population. The left section illustrates the cascade of allowed collisional transitions, while the right section represents the one-step collisional jump from the $\boldsymbol{E_p}$ level to the $\boldsymbol{E_u}$ level. The variable $\boldsymbol{n}$ denotes the ordinal number of the transitions: for the ground level, $\boldsymbol{n = 1}$; **n = 2** corresponds to the $\boldsymbol{E_u}$ level for the 548.82 nm and 622.13 nm generations, and so on. The last transition n **= 21**, represents the $\boldsymbol{E_p}$ level. **EI** collisions involving energy loss of excited atoms are discussed. In the first case, the cascade transitions follow the sequence $\boldsymbol{n = 24 \rightarrow n' = 23}$, $\boldsymbol{n = 23 \rightarrow n' = 22}$, continuing down to $\boldsymbol{n = 3 \rightarrow n' = 2}$.

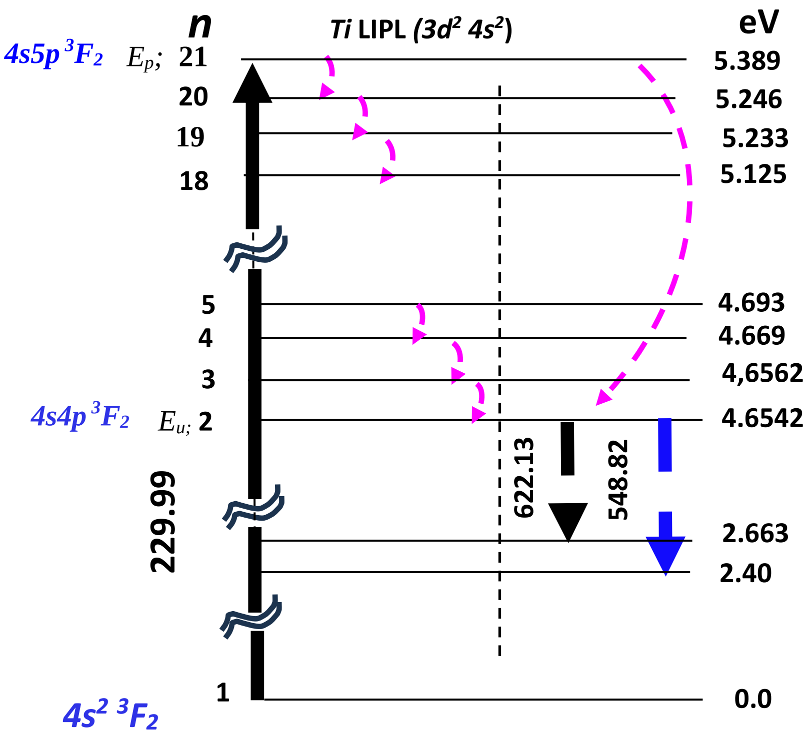

Figure 2. *The scheme of the Ti LIPL under pumping at 229.99 nm*
The left part presents the cascade of the allowed collisional transitions; the right part is the one-step collisional jump from the E_p level to the VIS generation E_u level

The rates coefficient $\beta^{mix}_{n\text{-}n'}$ (in cm^3/sec) for transitions between states n – *n'* (*n* > *n'*) is determined as follows [8,9]:

$$\beta^{mix}_{n,n'} = 4\pi\alpha_0^2\upsilon_e\left(\frac{I_H}{k_BT_e}\right)^2 3f_{n,n'}\psi_{n,n'}\frac{I-E_n}{I-E_{n'}}\,e^{-\frac{\Delta E_{n,n'}}{k_BT_e}} \quad , \qquad (2)$$

where indices *n* and *n'* denote the upper and lower states respectively, $\Delta E_{n,n'} = E_n - E_{n'}$. a_0 is Bohr radius, υ_e is the average electron velocity (proposing the υ_e Maxwellian distribution). I_H is the hydrogen atom ionization energy. $I = I_H Z^2$ is an atom ionization potential; *Z* is the atomic number.

$$\psi_{n,n'} = \frac{e^{-x_{n,n'}}}{x_{n,n'}} - E_i(x_{n,n'}), \quad x_{n,n'} = \frac{\Delta E_{n,n'}}{k_BT_e}, \quad E_i(x_{n,n'}) = \int_{x_{n,n'}}^{\infty}\frac{e^{-t}}{t}\,dt \quad , (3)$$

where $E_i(x_{n,n'})$ is the exponential integral function.

The oscillator strength $f_{n\ n'}$ is determined through the dipole moment matrix element, which depends on the initial and final states of the atom

$$f_{n,n'} = \frac{2m_e}{3\hbar^2}\frac{\Delta E}{e^2}\,|\langle\psi_n|\boldsymbol{d}|\psi_{n'}\rangle|^2 , \quad (4)$$

where m_e is the electron mass, $\hbar$ is the reduced Planck constant, *e* is the electron charge, and $\langle\psi_n|\boldsymbol{d}|\psi_{n'}\rangle$ is the dipole moment matrix element for the transition between the initial (ψ_n) and final ($\psi_{n'}$) wave functions.

Cascade collision rates Ac (probability in sec^{-1}) are:

$$A_c = N_e\prod_{j=21}^{2}\beta^{mix}_{n=j,n'=j-1} = N_e\left[\beta^{mix}_{n=21,n'=20}\,x\,\beta^{mix}_{n=20,n'=19}\,x\cdots x\,\beta^{mix}_{n=3,n'=2}\right], \quad (5)$$

where N_e is the electron density; $\beta^{mix}{}_{n=j,n'=j-1}$ is the coefficient for collisional transitions btween levels $n = j$ and $n' = j - 1$.

Jump-like probability A_{jamp} are:

$$A_{jump} = N_e \beta^{mix}_{n,n'} ; \qquad (6)$$

The results of the numerical estimation show that the probability of achieving the inversion population in the cascade of 21 transitions Ac **is about 0**, while the one-step jump probability between level ***n***=21 and level ***n'***=2 (**A_{jump}**) **is about 3.7 10^{10} sec^{-1}. This indicates that the jump-like collisions may dominate in the creation of the inversion population on the E_u level.**

This estimation is supported by the absence of the generation from intermedia levels which are populated during the cascade of collisions (see Fig. 3). The polarization observed in the 4-level generation with a large ΔE may further support the one-step collision process for populating the E_u level, as it is difficult to imagine.

References

[1] L. Nagli, M.Gaft, Lasing effect in laser-induced plasma plume, *Opt. Comm*., **354,** (2015) 330–332

[2] L. Nagli1, M. Gaft, I. Gornushkin, R. Glaus, Stimulated emission and lasing in laser-induced plasma plume, Opt. Comm. 378 (2016) 41–48

[3] L. Nagli, E. Stambulchik, M. Gaft, Y. Raichlin, Polarization effects in laser-induced plasma lasers based on elements from the 13th group, J. Appl. Phys. 129, (2021) 013103-1-6

[4] I. Gornushkin, R. Glaus, L. Nagli, Stimulated emission in aluminum laser-induced plasma: kinetic model of population inversion, Appl. Optics, 56 (2017) 695-70

[5] L. Nagli, M. Gaft, Y. Raichlin, Hanle effect in Ti Laser-Induced Plasma Lasers, Optics Communications 517 (2022) 128292-1-7

[6] L. Nagli, Polarization properties of the Laser-Induced Plasma Lasers generating according to the quasi-three-level scheme, Optics Communications 559 (2024) 130423-1-8

[7] L. Nagli, K. Kulikov Four-level generation in Laser-Induced Plasma LasersOptics Communications 583 (2025) 131665 1—11

[8] Ya. Zel'dovich and Yu. Raizer: *Physics of Shock Waves and High-Temperature Hydrodynamic Phenomena* (Dover Publications, Mineola, NY, pp. 382-421, 264-269, 2002)

[9] I. Gornushkin, A.Kazakov, Kinetic Model of Stimulated Emission Created by Resonance Pumping of Aluminum Laser-Induced Plasma, J. Appl. Phys. 121 (2017) 213303-1-11.

Towards the use of organic materials in the terahertz range

Petro Smertenko[1], Vadym Naumov[1], Zinoviia Tsybrii[1], Ihor Lysiuk[1], Daria Kuznetsova[1], Arnolds Ūbelis[2]

[1]Institute of Semiconductor Physics, National Academy of Sciences of Ukraine, Ukraine
[2]NSP FOTONIKA-LV, University of Latvia, Latvia

e-mail: petro.smertenko@gmail.com

Materials used in the terahertz (THz) range include conventional materials such as semiconductors: gallium arsenide (GaAs), indium phosphide (InP), and gallium nitride (GaN), which are used in devices for generating and detecting terahertz radiation; optical materials such as zinc cadmium telluride (ZnTe), gallium selenide (GaSe), and barium borate (BBO), which are used to generate and modulate THz waves; and plasmonic materials: metals (such as gold and silver), sometimes used to focus and amplify THz signals etc. [1-3]. Silicon technology is used as well [4]. Last decades nontraditional materials, like, for example, organic materials started to be used in this area of electronics. This is caused by the need for more efficient terahertz sources and detectors to handle propagation losses and the high cost of manufacturing and integrating THz systems. Organic Materials for THz Applications seems to have advances in such aspects: (i) flexibility and lightweight, (ii) low cost, (iii) scalability, (iv) tenable properties. Simultaneously there are some challenges with organic materials: (i) lower efficiency, (ii) material stability: (iii) charge carrier mobility [5, 6].

In this article, we compare different organic materials for generating, receiving and other devices in the THz wavelength range. One of the candidates for such application is heterocyclic amines like indoles, pyrroles, and quinolines, which sometimes used in organic photoconductors for THz generation and detection. These materials can be employed in photoconductive antennas, which convert optical pulses into THz radiation. The electrical properties of heterocyclic amines can be tuned to optimize their performance for THz applications. Some heterocyclic amines have the potential to be used in THz sensors and waveguides. Another candidate is carbazole and its derivatives which have shown significant promise in THz technologies due to their high electron mobility, optical properties, and easy functionalization. For instance, carbazole derivatives like 3,6-diphenylcarbazole and biscarbazole have been studied for their potential in THz generation. Their wide band gap and high electron mobility make them suitable for fast, efficient devices that can generate and detect THz radiation. Carbazole derivatives are also being investigated for use in THz modulators, which are devices that can control the amplitude, phase, or polarization of THz waves. Their ability to change their electronic properties under an external electric field makes them useful for modulating THz signals in communication systems. These materials could also play a role in flexible THz sensors or in THz detection systems where organic electronics offer advantages like flexibility, low cost, and lightweight characteristics. Both heterocyclic amines and carbazole derivatives can be chemically modified to tune their electronic and optical properties, making them very versatile for a variety of THz applications such as photodetectors, THz waveguides or modulators. Challenges related to efficiency and stability need to be addressed before these materials can be widely used in THz systems.

References

[1] Ukirade, N.A. (2025). A review on advancement of materials for terahertz applications. Next Materials, 6: 100479. https://doi.org/10.1016/j.nxmate.2024.100479

[2] Ling-Feng Shi, L.-F, et al. (2023). The perspectives and trends of THz technology in material research for future communication - a comprehensive review. Phys. Scr., 98: 065006. https://doi.org/10.1088/1402-4896/accd9d

[3] Lewis, R.A. (2019) A review of terahertz detectors. Journal of Physics D: Applied Physics, 52: 433001. https://doi.org/10.1088/1361-6463/ab31d5

[4] Marczewski, J. et al. (2018). THz detectors based on Si-CMOS technology field effect transistors – advantages, limitations and perspectives for THz imaging and spectroscopy. Opto-Electronics Review, 26: 261–269

[5] Kim, S.-J. et al. (2021). Nonlinear Optical Organic Crystals for Efficient Terahertz Wave Generation, Detection, and Applications. Adv. Optical Mater. 9: 2101019. https://doi.org/10.1002/adom.202101019

[6] Jazbinsek, M. et al. (2019). Organic Crystals for THz Photonics. Applied Sciences, 9(5): 882. https://doi.org/10.3390/app9050882.

ERDF project No. 1.1.1.5/2/24/A/004

Plasmonic crystals for THz applications

Vadym V. Korotyeyev, Pavlo Sai, Viacheslav V. Kochelap

Institute of High Pressure Physics PAS, Poland

and

V. Ye. Lashkaryov Institute of Semiconductor Physics, NASU, Ukraine

e-mail: koroteev@ukr.net

In the area of fundamental and applied condensed matter physics, there is a significant interest in the research related to the development of THz technologies focused on the elaboration of core elements of optoelectronic systems: generators, emitters, detectors, and modulators of electromagnetic radiation capable to operate in the frequency range of 0.1-10 THz. The relevance of this direction is primarily associated with the applied aspects of the widespread use of THz radiation in various fields, such as spectroscopy, including astrophysical measurements, 6G communications, medicine, environmental monitoring, security systems, explosives detection, etc. [1, 2]. Among the various areas of development of THz technologies, THz plasmonics is a new field with great prospects and achievements. This field studies the wide class of phenomena relating to the peculiarities of interaction of electromagnetic (em) waves of THz frequency range with collective oscillations of electron gas (plasmons) in low-dimensional structures and nanodevices on their basis [3, 4].

One promising platform for THz plasmonic systems is the plasmonic crystals (PCs) fabricated in the form of quantum well heterostructure covered by grating-gate metasurfaces (Fig. 1a). Such PC structures provide essential enhancement of THz light-matter interaction with particular resonant properties associated with different plasmonic modes excited in low-dimensional electron gas. PCs have shown enhanced performance as THz detectors [5] and hold potential for applications as THz emitters/amplifiers [6], and modulators [7, 8].

This thesis addresses to overview of recent experimental and theoretical studies of resonant interaction of plasmon excitation of 2D electron gas (2DEG) with THz electromagnetic waves in PCs. Particularly, several effects concerning a formation of different resonant-plasmonic phases of PC structures, 2D plasmon instabilities under metallic grating, magneto-plasmons, including non-linear effects of self-induced transparency of PCs by high-power picosecond pulses will be highlighted.

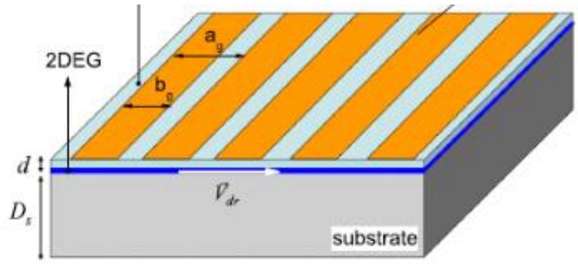

…

***Figure 1**. Sketch of metallic grating-based PC structure with 2DEG*

Acknowledgments: This research was supported by long-term program of support of the Ukrainian research teams at the Polish Academy of Sciences carried out in collaboration with the U.S. National Academy of Sciences.

References

[1] M. Tonouchi, Cutting-edge terahertz technology, Nature photonics 1(2), 97–105 (2007)

[2] J. Federici, L. Moeller, Review of terahertz and subterahertz wireless communications, J. Appl. Phys.107, 111101 (2010)

[3] T. Otsuji and M. Shur, Terahertz Plasmonics: Good Results and Great Expectations, IEEE Microw. Mag. 15, 43 (2014)

[4] M. S. Shur, Terahertz Plasmonic Technology, IEEE Sens. J. 21, 12752 (2021)

[5] V. Popov, D. Fateev, T. Otsuji, Y. Meziani, D. Coquillat, and W. Knap, Plasmonic Terahertz Detection by a Double-Grating-Gate Field-Effect Transistor Structure with an Asymmetric Unit Cell, Appl. Phys. Lett. 99, 243504 (2011)

[6] S. Boubanga-Tombet, W. Knap, D. Yadav, A. Satou, D. B. But, V. V. Popov, I. V. Gorbenko, V. Kachorovskii, and T. Otsuji, Room-Temperature Amplification of Terahertz Radiation by Grating-Gate Graphene Structures, Phys. Rev. X 10, 031004 (2020)

[7] P. Sai, V.V. Korotyeyev, M. Dub, M. Słowikowski, M. Filipiak, D.B. But, Y. Ivonyak, M. Sakowicz, Y.M. Lyaschuk, S.M. Kukhtaruk, G. Cywiński, W. Knap, Electrical Tuning of Terahertz Plasmonic Crystal Phases, Physical Review X, 13, 041003 (2023)

[8] P. Sai, V.V. Korotyeyev, D. B. But, M. Dub, D. Yavorskiy, J. Łusakowski, M. Słowikowski, S. Kukhtaruk, Y. Liashchuk, J.W. Han, C. Böttger, M. Mittendorf, Extreme Terahertz Nonlinearity of AlGaN/GaN-based Grating-Gate Plasmonic Crystals. preprint arXiv:2503.02562.

Lightguide fiber bundles

Jurģis Grūbe, Kalvis Alps, Mārtiņš Narels, Ivo Brūvers

Light Guide Optics International SIA, Latvia

e-mail: Jurgis.Grube@lightguide.com

Lightguide has developed an innovative fiber bundle end treatment technology – a stacked fiber bundle (SFB) that facilitates the efficient transmission of the laser light in the deep UV region and does it with minimal losses. Light delivery from a source to a destination can be achieved in several ways using fiber bundles. Lightguide has developed clad fused bundle (CFB) technology that allows high power (up to 6 kW) transmission with low losses in wide spectral regions; while also enabling shaping the bundle ends (the ends can be the same shape or different) in virtually any 2D shape. However, certain applications necessitate the transmission of shorter wavelengths, specifically in the deep UV spectrum (Nd:YAG IV and V harmonics), where existing bundle end technologies have limitations – mainly degraded performance over time and lower transmission.

A stacked fiber bundle uses carbon coated hydrogen loaded fibers, known for their solarization resistance, formed in a way that enables high transmission and durability when exposed to deep UV light over extended periods. SFB technology could be used in a number of applications requiring transmission of light at deep UV spectral regions. These applications are found in medicine, quality control, UV curing, process analysis, etc.

Keywords:
Fiber bundles, deep UV, laser application, carbon coated fibers, hydrogen loaded fibers, deuterium lamp, Nd:YAG harmonics.

References

[1] K.F.Klein, P.Schliessmann, E.Smolka, M.Belz, W.J.O. Boyle, K.T.V. Grattan, "UV-stabilized silica based fiber for application around 200 nm wavelength," Sensors and Actuators B, Vol. 38-39, pp. 305-309 (1997); https://doi.org/10.1016/S0925-4005(97)80224-9

[2] M. Huebner, H. Meyer, K.-F. Klein, G. Hillrichs, M. Ruetting, M. Veidemanis, B. Spangenberg, J. Clarkin, G. Nelson, "Fiber-optic systems in the UV-region," SPIE-Proc. BiOS'00, Vol. 3911, pp. 303-312 (2000); https://doi.org/10.1117/12.384918

[3] K. Alps, "Innovative fused end fiber bundle technology for high-brightness, irregular beam profiles," Proc. SPIE 12403 (2023); https://doi.org/10.1117/12.2648342

[4] K. Alps, I. Brūvers, J. Grūbe, and M. Narels, "Cutting-edge fused end fiber bundle technology for multi kW range applications," Proc. SPIE 12866, Components and Packaging for Laser Systems X, 1286603 (2024); https://doi.org/10.1117/12.3000484

[5] K.-F.Klein, C.P.Gonschior, D.Beer, H.-S.Eckhardt, M. Belz, J.Shannon, V.Khalilov, M.Klein, C.Jakob, "Silicabased UV-fibers for DUV applications: current status," SPIE-Proc., Vol. 8775, paper 8775-10 (2013); https://doi.org/10.1117/12.2020993

[6] J.Heimann, K.-F.Klein, C.P.Gonschior, Moritz Klein, G.Hillrichs, "Optical fibers for 355 nm pulsed lasers and high-power broadband light sources," SPIE-Proc. BiOS'13, Vol. 8576, paper 8576-19 (2013); https://doi.org/10.1117/12.2005146.

ERDF project No. 1.1.1.5/2/24/A/004

Conference is supported by the European Regional Development Fund Project **No. 1.1.1.5/2/24/A/004 "*ERA Chair in Astrophysics, Instrumentation, Ground Segment Technologies and Space Photonics at the University of Latvia*"**

Coming soon:

Photonics and Conference promoters:

Light Guide Optics International, SIA:
https://www.lightguide.com/about

Baltic Scientific Instruments, SIA:
https://bsi.lv/en

Cryogenic and Vacuum Systems, SIA:
https://cvsys.eu